1-1-2013

Investigation Of Physiochemical Properties Of A Novel Gradient Calcium Polyphosphate Bone Scaffold And Its Influence On Cellular Behavior

Liang Chen
Wayne State University,

INVESTIGATION OF PHYSIOCHEMICAL PROPERTIES OF A NOVEL GRADIENT CALCIUM POLYPHOSPHATE BONE SCAFFOLD AND ITS INFLUENCE ON CELLULAR BEHAVIOR

by

Liang Chen

THESIS

Submitted to the Graduate School

of Wayne State University

Detroit, Michigan

in partial fulfillment of the requirements

for the degree of

MASTER OF SCIENCE

2013

MAJOR: BIOMEDICAL ENGINEERING

_____

Advisor Date

ACKNOWLEDGEMENTS

I would like to especially thank Dr. Weiping Ren for granting me this great opportunity and support. I also thank Dr. Haward Mathew for his adviser and guidance on bioreactor system design and experiments.

TABLE OF CONTENTS

LIST OF TABLES

LIST OF FIGURES

Chapter 1 General Introduction

1.1 Basic Bone Biology and Regeneration

Bone is a highly mineralized connective tissue that is able to support human body and maintain mineral homeostasis[1]. Macroscopically, bone tissue can be classified into compact bone (cortical bone) and spongy bone (trabecular bone)[2]. Compact bone is mainly responsible for supporting and protecting. It is formed by plenty of osteons with longitudinal Haversian canal passing through the center[2]. And each osteon is connected by Volkmann's canal. The Haversian canal and the Volkmann's canal form the network for bone's nutrition supply and signal transduction[1, 2]

Spongy bone is a light weight, highly porous tissue where riches in blood vessel and contains bone marrows. Usually it locates inside of compact bone or at both ends of long bone. The unit structure of spongy bone is trabecula. The main blood vessel, lymphatics and nerve fibers go through the center of spongy bone. Red bone marrow full filling pores of the spongy bone. Therefore, the spongy bone has the function of supply nutrition for bone cells, hematopoiesis, and keep mineral balance in body. The coating of bone is named periosteum which is a highly vascularized connective tissue. Not only can it connect one bone tissue with anther or with muscle tissue, but also has the ability to produce bone during body development and bone healing because amounts of bone cells accumulate at inner layer of periosteum [3, 4].

The extracellular matrix of bone tissue is different from other connective tissue, because it is highly mineralized. It contains 65% of inorganic matrix and 35% of organic matrix[2]. The major component of minerals matrix is hydroxyapatite [$Ca_{10}(PO_4)_6(OH)_2$]. The organic matrix is composed of type one collagen and more than 200 kinds of noncollagenous proteins, such as fibronectin, osteopontin and osteocalcin [2]. This kind of organic matrix is important for bone

cells adhesion, proliferation, differentiation, accumulation and signal transduction of growth factor.

There are several types of bone cells related to the bone remodeling, such as mesenchymal stem cells (MSCs), osteoblasts (OB), osteocytes (OC), osteoclasts, and chondrocytes[1]. The mesenchymal stem cells located in bone marrow are small, long and thin cells with large nucleus[5]. They have great capacity of self-renewal and can differentiate into adipocytes, chondrocytes, osteoblasts, adipocytes, hepatocytes, and pneumoncytes. In the vascularization area, the mesenchymal stem cells would differentiate into osteoblasts; while they are under the non-vascularization area, they would form chondrocytes [2, 5-7]. The osteoblasts, immature bone cells, produce osteoid matrix which is mainly composed of type I collagen, alkaline phosphatase, and other proteins [8]. After osteoblasts are trapped and deposit in the bone matrix, they eventually develop to mature bone cells, osteocytes. Like osteoblasts, the osteocytes can secrete hydroxyapatite, calcium carbonate and calcium phosphate bone matrix[2, 8].Besides, they are very sensitive to mechanical strain and can also secrete many growth factors to help cells proliferation and differentiation. Chondrocytes originated from mesenchymal stem cells are related to cartilage formation [9]. The osteoclasts are large and multinuclear cells which is important for bone degradation and re-sorption. There are several specific cell markers for osteoclasts like Receptor Activator of Nuclear Factor κ B (RANK) [2]. It also can be regulated by many hormones such as parathyroid hormone and calcitonin [2].If there are some imbalances between these factors, it can lead to several diseases like osteoporosis. Therefore, it is important to keep the equilibrium between bone formation and bone re-sorption.

Many growth factors and transcription factors participate in osteogenesis such as bone morphogentic proteins (BMP), Cbfa/Osf2, alkaline phosphatase (AKP), fibroblast growth factor

(FGF) and vascular endothelial growth factor VEGF [1,2, 10-12]. For example, BMP is pivotal for bone building, remodeling, and healing. So far, BMP have been classified into 7 types. Generally, BMP through binds to bone morphogentic protein receptor (BMPR) leading to BMPR phosphorylated which would cause cascade phosporylating sub signaling protein such as Smad1 to transduce bone formation information[2]. Because BMP can instruct MSCs differentiate into chondrocytes and osteoblast to form cartilage and bone, it provide an potential function for many pathological treatment such as BMP defection disease, spinal fusion, bone fracture surgery, and bone regeneration. Alkaline phosphatase is an enzyme and more effective in an alkaline environment to dephosphorylate these phosphorylated proteins. It is the by-product of osteoblasts. It can be tested in blood as an indicator of osteoblasts activity. While it is at high level of blood, bone may be under growth situation. However, if it is quite high which may also mean some disease occurs like chronic myelogenous leukemia, it is a pretty lower level can lead to bone deformities.

Intramembranous ossification mainly responsible for forming skull and flat bones[2]. During the intramembranous ossification, neural crest-derived mesenchymal cells recruited by BMPs, cytokines and α-TNF family accumulate around vascularized area, and proliferate forming condense nodules. Then these mesenchymal cells differentiate into osteoblasts. Osteoblasts, bone forming cells, secrete a collagen-proteoglycan matrix which is able to bind calcium salt. The osteoid matrix induces more and more mesenchymal cell aggregating and differentiating around it, as a result, more and more osteoblasts deposit around the osteoid matrix. Some osteoblasts are entrapped into the matrix and develop to mature bone cell—osteocytes accidentally. As calcification proceeds, bony spicules formed. With the spicules growth, mesenchymal cells and osteoblasts still deposit into the spicules. Furthermore, spicules located

closely fuse together form the trabecula. The trabecula network is called woven bone which is characterized by haphazard organization of collagen fibers and is mechanically weak[6]. Later the entire region of woven bone is surrounded by periosteum originated from mesenchymal cells. In inner side of periosteum, osteoblasts continue secrete the osteoid matrix and develop to osteocytes. Therefore the layers of bone formed. Besides, the previous vascular area is developed to Haverian canal.

The secondary bone formation process is called endochondral ossification[2]. It first forms cartilage following replaced by osteoblast to form sponge bone. The whole process can divided into five steps. Firstly, MSCs aggregate and differentiate into chondrocytes with the help of lots growth factors, and chondrocytes form cartilage model. Secondly, because of little blood vessels in these non-vascularized areas and the growth of cartilage model, these chondrocytes are under hypertrophic environment which would lead to the apoptosis of chondrocytes. Thirdly, the formation of the first ossification center, as the apoptosis of chondrocytes, arteries enter into diaphysis which would bring osteoblasts and osteoclasts. With the entrance and growth of osteoblasts, they would form trabecular, and eventually create sponge bone by secreting osteoid and mineralizing cartilaginous matrix. For osteoclasts, they degenerate cartilaginous matrix under the regulation of two hormones, parathyroid hormone (PTH) which release calcium into blood and calcitonin which bring calcium back to bone, to form medullary cavity in the center of the diaphysis. Fourthly, when these blood vessels enter the end of each bone, the secondary ossification center occurs in epiphysis. The secondary ossification center goes through the same process as the first ossification center to form sponge bone. The secondary ossification center can divide into six zones. The zone of reserve cartilage is a hyaline cartilage zone contains lots small cells; in the zone of cell proliferation (ZP), chondrocytes cells are also small and arrange in

columns which have strong mitotic activity[2]; in zone of cell and lacunar maturation and hypertrophy enlargement (ZH), chondrocytes grow, have a larger size than them in ZP, and go through apoptosis process; in zone of calcification (ZC), chondrocytes die and mineralizing bone matrix which can use basophilic staining to distinguish it with other zones; zone of cartilage removal and bone deposition is among ZC. The last step is the articular cartilage and epiphyseal plate form. This place is very sensitive to cushion and allows the bone to continue growth of sponge bone in adults.

1.2 Musculoskeletal disorders and injuries

Nowadays, several hundred million patients suffered from musculoskeletal disorders and injuries all around world, and this number may be double by 2020 as ageing[2].In United State, 50% of the people aged over 65 are suffered from chronic joint disease. And half of women and a quarter of men aged over 50 will experience osteoporotic fractures[2] which account for three hundred thousand hip fractures, seven hundred thousand vertebral fracture and other fractures. It will directly cost 18 billion in treatment. In addition, a large number of severe bones defects will be caused by war and accident per year. Furthermore, other musculoskeletal diseases such as spinal disorder, osteoporosis, osteoarthritis and cancers will impact bone's function. Moreover, the bone disorders become more and more severe as the obesity and ageing. Therefore, bone regeneration strategies have attracted attention.

1.3 Current Bone Regeneration Strategies

Traditionally, the bone regeneration therapies are autologous or allogeneic transplantations and treat by metals or bone cements [13-15] . Autologous transplantation applies bone substitutes sourced from a patient's own bones in order to supply mechanical strength and maintain ostergenesis, osteoinduction and osteoconduction in bone defect[16]. The autografts are the ideal bone grafts, but it is limited by supply and pain and /or morbidity in harvest site [15,

17].The morbidity after orthopedic surgery using an autograft from the iliac crest is close to 30%[18]. Furthermore, the expenditure of this surgery is expensive[17]. And usually, patients need receive a long time of medical care after the surgery.

In order to overcome the drawbacks of autografts, allografts, donated from other people, have been widely applied. For example, recent years, more than a million allografts were transplanted in bone injured individuals[2]. The allografts with various shape and size satisfy the requirement of the bone grafts. In addition, the patients no longer need to suffer from the compliments of harvest site. Nevertheless, the amount of allografts still cannot satisfy the need. Moreover, the allografts transplantation may potentially transmit diseases from the donors. The grafts' quality, mechanical strength, osteogenesis, and osteoinduction, also are impacted after serializing and freezing proceeds [2, 16, 17].

Tissue engineering may be a promising solution to overcome these drawbacks for the bone regeneration strategy. It combines the principle of life science and engineering to induce bone tissue regeneration[19]. The bone tissue engineering involves three factors: cell, bone scaffold and bioactive agents[20]. The bone scaffolds mimicking nature bone structure integrate with bioactive agents to stimulate cell growth, vasculature and nerve formation [2, 21]. Consequently, it is able to promote tissue regeneration and sustain the mechanical stress during bone regeneration[21].

1.4 Bone graft

The artificial bone graft is a significant factor in tissue engineering. Structure, materials and fabrication techniques can decide the properties of bone scaffold. An ideal bone scaffold should be non-toxic at least[2]. Before usage, the scaffolds need to be sterilized. Meanwhile, biocompatibility is second requirement for an ideal bone scaffold. The bone scaffold with good biocompatibility can avoid undesired rejection by host tissue[22]. Usually, the biocompatibility

of bone scaffold can be interpreted at three levels: (1) Blood protein interaction[23]. After implantation, the scaffold contacts with the blood protein firstly. This interaction can affect cell attachment and host response to the scaffold [23, 24]; (2) Local host response. The bone scaffold will be degraded through corrosion [25, 26], hydrolysis [27, 28], as well as enzymatic reaction. As a result, degradation products may induce unwanted response like inflammation and immunological reaction at the transplant site[29]; (3) Systemic effect. If the degradation products were not eliminated, it would transport to whole body through circulation, and cause severe immunological response[29]. Therefore, the biocompatibility can lead the grafts to succeed or failure. In addition, not only the material of scaffold should be biodegradable, but also the degradation rate should keep in the similar speed with bone remolding rate. Since the scaffold can temporally provide the bone's function until the new bone formed. Moreover, the bone scaffold should be a poriferous structure. Since porosity, pore size and pore interconnection of the scaffold closely relates to cell attachment, osteogenesis and mechanical strength [30, 31]. A scaffold with larger pore size, higher porosity and pore interconnection is benefit to nutrition and oxygen transportation and cell ingrowth. Previous research showed that osteogenesis occurs at the area with large pore size (>350μm) and high porosity in vivo [32]. They also found that capillary cannot grow inside the pore with the size less than 200μm [32, 33]. As a result, these areas usually proceed chondrogenesis. Besides, the larger pore size, higher porosity and pore interconnection result the roughness surface of scaffold which improve cell attachment, proliferation and differentiation. However, this structure impacts the mechanical strength and increase the biodegradation rate. In conclusion, a good bone scaffold should have appropriately porosity to maintain the balance between osteogenesis and mechanical strength. Furthermore, as mentioned above, the bone scaffold should sustain mechanical loading. The mechanical strength

of nature bone relates to harvest site, gender, age, sample preparation and test environment. So it is difficult to decide the bone strength. Generally, the spongy bone can bear 2-12MPa strength, and the cortical bone can stand 200MPa [34]. Overall, a desired bone scaffold should mimic the nature bone structure and properties [35].

Bone grafts materials can affect biocompatibility, degradation rate and osteogenesis process. Generally, materials can be classified into three types: natural polymer, synthesis polymer and ceramics. Natural polymers, like collagen, chitosan and hyaluronan, are designed to mimic bone extracellular environment[36]. They have desired biocompatibility and can interact with cells[36]. And they are biodegradable but the degradation rate is difficult to control[36]. The more important is that the mechanical strength of this scaffold is weak. The second type of the material is synthesis polymers, such as PCL, PLA, PLA-PEG and PLGA. The degradation rate and mechanical properties are easier to control for this type material through change chemical bonds as well as the repeat units of polymer[2]. However, the degradation products are toxic sometimes which may cause inflammation and immulogical response[2].

The last type of material is ceramics which mimics the mineral composition of nature bone[37]. In general, the ceramics scaffolds can stand high mechanical loading and have good biocompatibility [37, 38]. The extensively used ceramics materials are hydroxyapatite (HA), tricalcium phosphate (TCP), bioactive glasses, and mixed calcium phosphate (MCP, mixed by HA and TCP) [39]. As the bone substitute materials, they can be applied in particulate and bulk form. For instance, HA has similar chemical structure and crystallography with carbonated apatite in nature bone. It is also the maximum inorganic component in ECM of bone tissue. HA can be used as particulate to fill the defects with irregular shape, like dental implantation. Simultaneously, it is used as bulk form when replacement of defected bone caused by trauma or

disease is need. The major drawback of these materials is comparatively low strength properties. Some researchers found that the mechanical strength of HA and TCP scaffold were less than 2MPa and without any strength in tension [40, 41]. Besides, the degradation rate is hard to control. For example, Hench LL *et al.* discovered that the degradation rate of HA was much longer than the bone growth rate which was not benefit to osteoinduction and osteoconduction [42]. Consequently, better bone grafts materials should be investigated for satisfied requirements.

Chapter 2 Physiochemical characterization of gradient vs. homogenous SCPP scaffolds

2.1 Introduction

2.1.1 Calcium polyphosphate as bone grafts material

Recently, more and more attentions have been focused on calcium polyphosphate, because it shows controllable biodegradation, desired biocompatibility and better mechanical strength. Calcium polyphosphate (CPP, $[Ca(PO_3)_2]_n$) has lower Ca:P ratios (0.5) than HA (Ca : P=1.67) and TCP (Ca:P=1.5) [39]. Therefore, CPP with low Ca:P ratios can forms a chain-like polymer which is linked by oxygen bridged phosphate tetrahedral [39, 43] (Figure 1). Each bridging oxygen atoms within the CPP structure represent a possible center for hydrolysis. The degradation product is calcium orthophosphate, a naturally occurring metabolizable substance. That is the reason for its good biodegradation and biocompatibility. Additionally, the CPP can bear higher mechanical loading than other calcium phosphate materials. Pilliar et al. reported that a CPP scaffold with 30% porosity can stand 24.1MPa strength during compression test [39]. Many researches have investigated the potential application of CPP for bone tissue engineering. The first reported research was using CPP to replace the defect in rat femurs[44]. Researchers found no adverse host response to implanted CPP scaffolds 4 weeks after [44]. Later other research group used the CPP to restore mandibular crestal bone in dogs[45]. 4 months later, after

sacrifice, they found that compared with autografts the CPP scaffolds significantly stimulated the bone ingrowth. In conclusion, the CPP could be a suitable material for bone substitute.

2.1.2 Gradient porous bone scaffold

Conventionally, the bone scaffolds have a uniform/ homogenous structure, dense structure or porous structure. However, as we know, nature bone is not a uniform tissue which consists of spongy bone and cortical bone with different pore size and porosity. For this reason, functional gradient scaffolds have been designed and studied about twenty years. The gradient scaffolds are purposely designed with continuous change microstructure [46]. The pore size, porosity and interconnectivity can be all graded throughout of the scaffold. According to application, the gradient scaffold can be formed in different shapes. For example, it can be cylindrical with dense core and porous layers which is able to stand high mechanical strength [46]; also it can be rectangular which have dense bottom-porous top or porous top-dense center and bottom[46].

Comparing to homogenous scaffold, one of the advantages of the gradient structure is functional layers. Dense bone scaffold has high mechanical strength but is not good for bone ingrowth; while the porous scaffold benefits bone in growth but has weak mechanical strength. So the gradient scaffold can overcome the drawbacks of these scaffolds. Since porous layers are suitable for cell attach and growth; dense layers have high mechanical strength. Besides high interconnectivity on porous layers performs the function of vascular canals in bone tissue which benefit to nutrition transport. In addition, the grade pore size benefits to grow different types of cells and form different tissues. For example, the chondrocyte prefers grow on the area with pore size from 70 to 120 μm; and bone regeneration usually happens on larger pore size (100-400 μm) [47]. In general, the gradient scaffold provides different microenvironment for various cells ingrowth. The gradient structure also is better to match the bone growth rate. Porous layer allows

the initial bone ingrowth, and later the longer time remodeling will happens on the layer with small pore size.

2.1.3 Fabrication of gradient scaffold

The processing methods for homogenous scaffolds fail to apply on gradient scaffold completely. Thus, fabrication of gradient scaffolds is a new challenge. Currently, several methods have been developed, such as vacuum infiltration, pulsed electric current sintering, pressure filtration of mixed particles, electrosparying, centrifugation of suspension and freeze drying, etc. [46].Some of them are able to fabricate graded pore size, but unable to form good interconnectivity and porosity; others may enable to form good interconnectivity and high porosity, but fail to control the structural regularity. For example, the pressure filtration of mixed particles usually applied to make graded hydroxyapatite scaffold. It mixes hydroxyapatite slurry with a compositional gradient carbonaceous particle suspension during filtration process. The dried and consolidated mixture is sintered, forming a gradient porous scaffold. This method can control the porosity, but fail to form a gradient pore size structure and high interconnectivity because the carbonaceous particles are in uniform size [48]. The elctrospraying method can form the gradient scaffold with high porous interconnectivity. It can use ceramic droplet such as hydroxyapatite to pass through an electric field and to deposit on a porous template like polyurethane sponge [49]. After that, the ceramic structure is sintered to burn off the template. The limitation of this method is uncontrollably regular structure.

In the first part of this study, we developed a novel fabrication method of gradient scaffold CPP scaffold, gravity sintering. We mixed and compressed finely grounded amorphous calcium polyphosphate granules with porogen, stearic acid, with gradient size in solid form. And later the scaffolds were sintered in a furnace for 8 hours and 20 minutes in order to evaporate the stearic acid and form the gradient pores. Based on the principle of fabrication, this method can

control pore size, porosity, and porous distribution and should have good interconnectivity. In order to testify this novel fabrication method and to study the gradient scaffold, the properties of these scaffolds were studied to determine how the distribution and variation of porosity affects the structure of the scaffolds compared to homogeneous scaffolds.

2.2 Materials and Methods

2.2.1 Materials

Calcium phosphate monobasic monohydrate ($Ca(H_2PO_4)_2.H_2O$), Serial acid, PVA solution (15%, w/v, Mw 70,000), calcein were obtained from Sigma-Aldrich (USA), Sodium EDTA and Muffle furnace were from Fisher Scientific (USA). Microplate reader was obtained from BioTek (USA). Manual pellet-press was from Carver (USA), SEM was purchased from Hitachi S-2400 (Japan), Gold Sputter was from Effa Coater (USA), MicroCT (Scanco Viva CT 40) was from Scano Medical (Switzerland). Universal servohydraulic test machine was from Instron (USA)

2.2.2 Preparation amorphous calcium polyphosphate (ACPP) granule

The amorphous calcium polyphosphate (ACPP) originated from the calcium phosphate monobasic monohydrate through calcining procedure. Briefly, around 100g the calcium phosphate monobasic monohydrate was pressed into a 100ml ceramic cup and put into a furnace for calcining. The procedure of calcining was as followed: (1) temperature in the furnace increased to 500°C in 40mins; (2) material was calcined at 500°C lasting 10h; (3) temperature increased to 1200°C in 30mins; (4) material stayed and melted for 1 h at 1200°C. After that, the melting material was poured on ice immediately, which called ice squash. Since the temperature falling down quickly, the crystallization process of the material was not complete. Finally, the ACPP products were harvested. The ACPP crystal were manually grounded and sieved into ACPP granule with the particle size less than 75μm.

2.2.3 Preparation of Gradient and Homogenous scaffold

Basically, the scaffold was made through sinter method. For gradient scaffold, the finely grounded ACPP powder (<75μm) was mixed with four gradient sizes of stearic acid, which was used as porogen and would be evaporated at high temperature, the size of stearic acid x>300μm, 300>x>250 μm, 250>x>75 μm and x<75 μm. The ratio of ACPP to stearic acid was 4:3 (Table 1). The four gradient layers of material were pressed into a cylindrical tube respectively and were compressed under a loading pressure of 70 tons. At the last, the scaffold was sintered by furnace for 8 hours and 10 minutes. The gradient scaffold in cylindrical shape with1cm diameter and with 0.9 cm height was made (Figure 2).

For the homogenous scaffold, the procedure was the same. The only different step was when adding the material into the cylindrical tube make sure the four layers' material were mix evenly.

The sinter procedure was as followed:

$$100°C \xrightarrow{30min} 300°C \xrightarrow{3\ h} 300°C \xrightarrow{100min} 800°C \xrightarrow{3\ h} 800°C \xrightarrow{\text{Over night}} \text{cooling down}$$

at room temperature; Since the materials were cooling down naturally, the crystallization process was completed. Thus the ACPP was formed to crystal CPP which has higher mechanical strength.

2.2.4 Investigate the structural properties of Gradient and Homogenous scaffolds

The structure properties were tested by MicroCT and SEM. Each scaffold was scanned with the Scanco VivaCT 40 using a voltage of 55 kVp and a current of 145 uA at 10um resolution. A cylindrical volume of interest was selected (100 slices) for each of the four layers within the gradient scaffold and 400 slices were selected for the homogeneous scaffold. An optimal threshold of 370 was determined. The morphology of the scaffolds was determined using software from the manufacturer to measure the average wall thickness (Tb.Th), average pore size (Tb.Sp), porosity, pore size distribution and interconnectivity.

Additionally, each gradient and homogenous scaffold was gold-coated by using Sputter coater. Morphologies were viewed by SEM at the operation of 25kV accelerating voltage.

2.2.5 Mechanical Properties

Unconfined, uniaxial compression test was applied to test the mechanical strength by universal servohydraulic test machine. The maximum deformed strain was 0.5 with the compression speed of 0.01mm/s. The maximum mechanical strength=maximum force/ the cross section area of scaffold. Each sample was set in triplicate.

2.2.6 In vitro degradation study

In vitro degradation study was measured by released Ca^{2+} concentration. The scaffolds were incubated in PBS at 37°C for sixteen days separately. Aliquots of PBS were collected to measure the Ca^{2+} concentration at different time points and replaced by fresh PBS. The Ca^{2+} concentration was measured as followed: calcein solution (1mg/ml) was added and reacted with the Ca^{2+} released in the PBS to form a green-yellow color. Na_2-EDTA solution was added to chelate with Ca^{2+} to form a green color. The microplate reader was used to measure the fluorescent intensity (FI sample) of the solution. At the same time, fluorescent intensity of blank group (FI blank) was measured as well. The Ca^{2+} concentration = ((FI sample-FI blank)/(-5000))^1.5. The continuous degradation curve was plotted.

2.3 Results

2.3.1 Gradient and homogenous scaffolds structure by MicroCT scanning

A three dimensional rendering of homogenous and gradient scaffolds is shown in Figure.3.The average pore size of the homogenous scaffold was 0.21mm. For the gradient scaffold the pore size decreased from first layer (0.38mm) to fourth layer (0.08mm). Also the porosity of the gradient scaffold was decreased from 65% (first layer) to 13% (fourth layer). And the porosity of homogenous scaffold was 32% (Table 1). The pore size distribution differed

among the layers of the gradient scaffold. In the first layer, a high percentage (63%) of the pores was greater than 300um in size. In the second layer, 72% of the pores fell within 75 – 250um in size. The pore size continued to decrease in the third layer, and by the fourth layer 68% of the pores fell below 75μm in size (Figure 4). The percentage of pores that were connected to the outside environment through 20μm openings was 100%, 93%, 76%, and 46% for layers 1, 2, 3, and 4 of the gradient scaffold. These percentages dropped to 89%, 15%, 11%, and 14% for 200μm openings. As for the homogeneous scaffold, 79% of the pores were connected to the outside environment through 20μm openings and 10% for 200μm openings (Figure 5).

2.3.2 SEM scanning of gradient and homogenous scaffold

Both the gradient and homogenous scaffolds exhibited 3D interconnected pore structure (Figure 6). For the gradient scaffold, the majority pores on the top were open pore (connected pore), and most of the pores had larger inter space. The middle and bottom layers exhibited a denser structure; not only the pores became smaller, but also became isolated. Overall, the pore size and interconnectivity of gradient scaffold declined from the top to the bottom the interconnectivity of the structure declined. Meanwhile, for the homogenous scaffold, the pore size and interconnectivity of pores kept evenly distribution.

2.3.3 Mechanical property

Generally, the homogenous scaffold can endure higher mechanical stress (9.03MPa) than the gradient scaffold (6.12MPa) (Figure 7 -8). And the maximum strains of homogenous and gradient scaffolds were 0.024 % and 0.25% respectively (Figure 7-8). At the same time, the Young's Modulus has been calculated based on the stress and strain curve. As the same, the Young's Modulus of homogenous scaffolds (6MPa) was higher than the gradient scaffolds' (3.5MPa) (Figure 9a). The stress distribution of homogenous scaffold uniform distributed

through out of the scaffold; while in gradient scaffold, the stress loading mainly focused on the middle and bottom of the scaffold which was the area with smaller pore size (Figure 9b).

2.3.4 In vitro degradation study

The degradation of gradient and homogenous scaffold exhibited similar pattern and speed. Both of them have high degradation speed at beginning and kept stable after sixteen days (Figure 10)

2.4 Discussion

The novel gravity sintering method was easy to processing. After sintering, the solid and compressed amorphous CPP materials were recrystallized, forming a harder structure. Using the graded size of porogens was easy, controllable to form gradient pore size and different porosity. Our results showed that the gradient scaffold had three-dimensional interconnected pore structure. The four functional layers of the gradient scaffold were obviously (Figure 3). The 1st t and 2nd layers mainly distributed by open pores (>250μm), resulting in higher porosity (65%, 55%) and interconnectivity. Thus, it could provide larger space for cell ingrowth and osteogenesis because osteogenesis prefer happening in the area with large pore size (>300μm). The wider connection space between pores provided a favorable matrix for cell migration and/or growth into the pores. While the 3rd and 4th layer exhibited dense structure with small pore size and porosity. This structure mimics the structure of nature bone. When the scaffold implanted into body, the layers with larger pore size and porosity enable the cell ingrowth, nutrition and oxygen transportation; meanwhile the dense layers can support sufficient mechanical strength.

The mechanical strength is the other important factor for the bone graft. As mentioned above, the calcium polyphosphate can stand higher mechanical loading than some other materials like HA and TCP. In this study, the maximum mechanical strength of gradient and

homogenous scaffold was 6.5MPa and 9MPa respectively. The stress-strain relation of gradient scaffold was different from the homogenous one. Since the first and second layers of gradient scaffold has weak mechanical strength. As the results, the structure of these two layers damaged firstly, and then it with the 3rd and 4th layer stood the loading force together. In the Figure 8, the strain percentage did not decrease after compression, indicating that the structure of gradient scaffold was damaged to some extent. And the 3rd and 4th layers of the gradient scaffold bear the most mechanical strength (Figure 9b). In order to improve the mechanical strength, we may try to use much finer CPP powder (<38μm in diameter). Since densification rates are inversely proportional to powder size [50]. Pilliar et al. compared the mechanical strength of coarse powder sample (particle size: 150-250μm) with fine powder sample (106-150 μm)[39], and found the fine powder scaffold can bear four times higher loading force than the coarse powder scaffold. So finer powder scaffold can bear higher loading force.

Biodegradation rate is crucial to bone graft because it can impact osteogenesis. The two type of scaffold exhibited similar degradation trend and speed (Figure 10). It means that the different structure of scaffold cannot change the degradation rate of the material. The degradation rate of CPP can be controlled by many factors. For example sintering procedure (time and temperature) enable to affect $(PO_4)^{3-}$ chain length which is related to the degradation rate. In addition, crystal structure, degradation medium and porosity can change the degradation rate.

In general, the novel gravity sintering approach had successfully established gradient CPP scaffold. The gradient scaffold has clearly four functional layers with gradient pore size. The reduction of mechanical strength of gradient scaffold can be improved by using finer powder. Besides, the biodegradation rate was controllable. Thus, the gradient scaffold with its unique

structure has many advantages than the homogenous scaffold. Then we compared the cell behaviors cultured on the gradient and homogenous scaffold.

Layers	Materials		
	ACPP powders (g)	Stearic Acid (g)	Stearic Acid size (x, μm)
1st layer	0.225	0.15	x>300
2nd layer	0.225	0.15	250<x<300
3rd layer	0.225	0.15	75<x<250
4th layer	0.225	0.15	x<75

Table 1 Materials component for gradient scaffold

Sample	Porosity (%)	Tb. Th (mm)	Tb. Sp (mm)
Gradient Layer 1	65%	0.21	0.38
Gradient Layer 2	55%	0.10	0.13
Gradient Layer 3	32%	0.11	0.10
Gradient Layer 4	13%	0.13	0.08
Homogeneous	32%	0.12	0.21

Table 2 Scaffold morphology

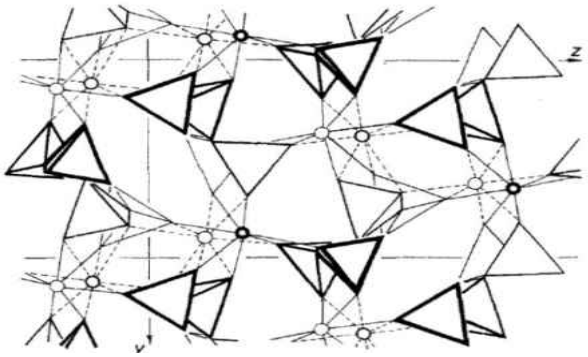

Figure 1 Projection of the CPP structure along **x.** Dashed lines is (Ca(1)-Ox)-polyhedra; Continuous lines is (Ca(2) – Ox)-polyhedra

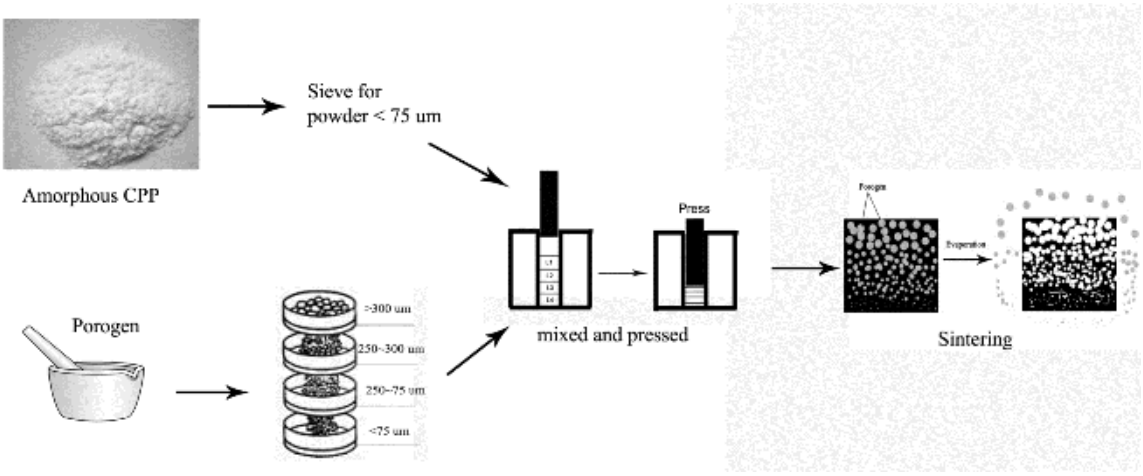

Figure 2 The fabrication process of gradient and homogenous scaffolds

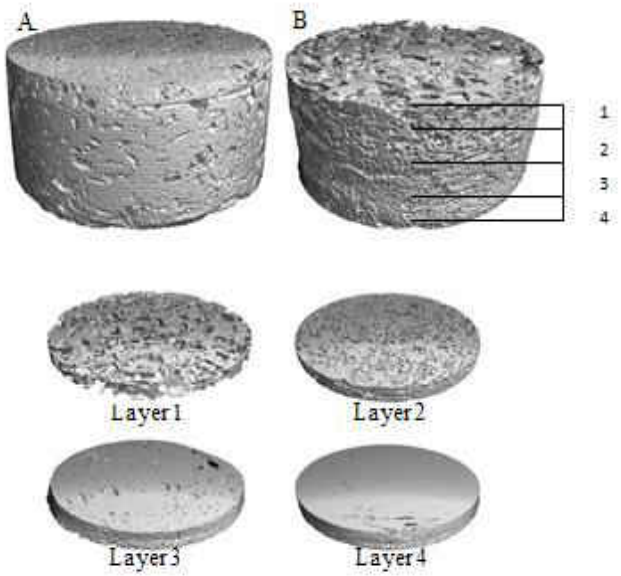

Figture 3 3D rendering homogenous (A) and gradient (B) scaffold showing the different layers within the gradient scaffold (C).Layer 1: >300μm; Layer 2: 250-300μm; Layer 3: 75-250μm and Layer 4: <75μm.

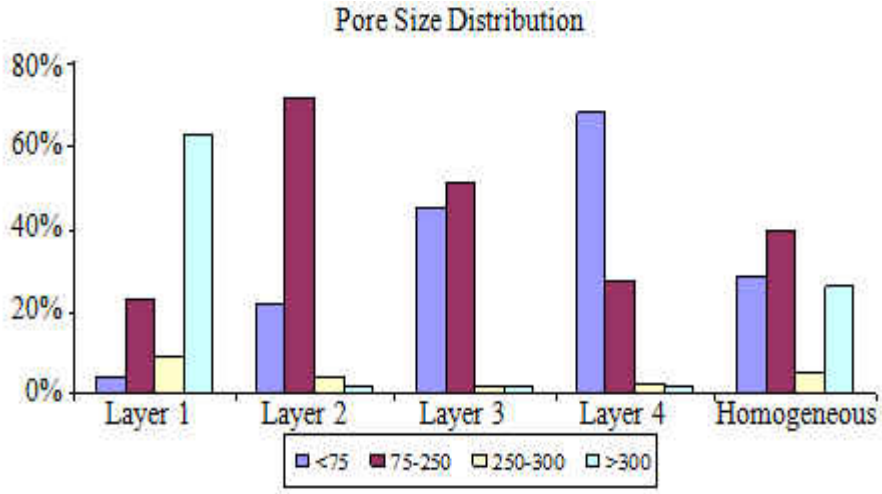

Figure 4. Distribution of pore size

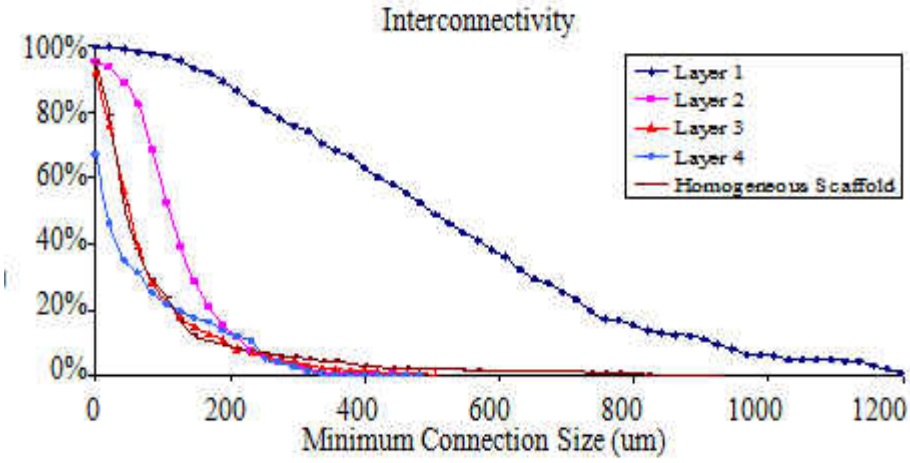

Figure 5 Interconnectivity

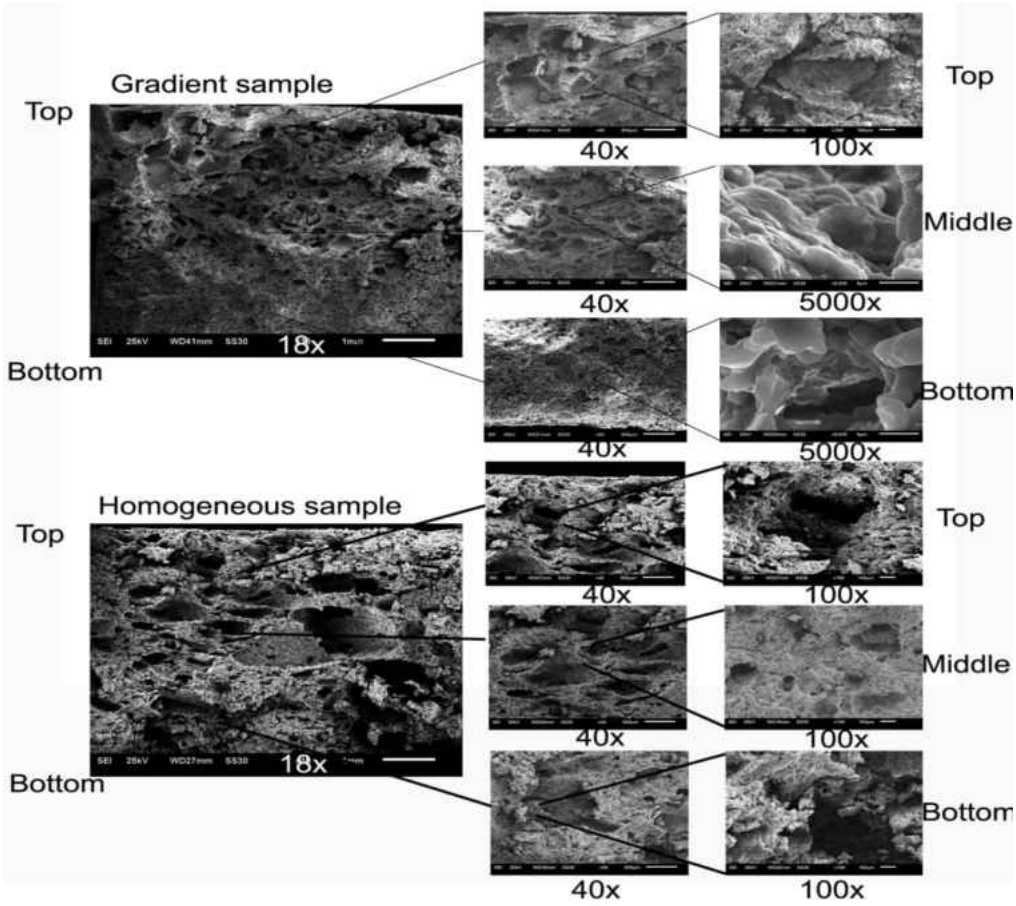

Figure 6 The SEM image of gradient and homogenous scaffold

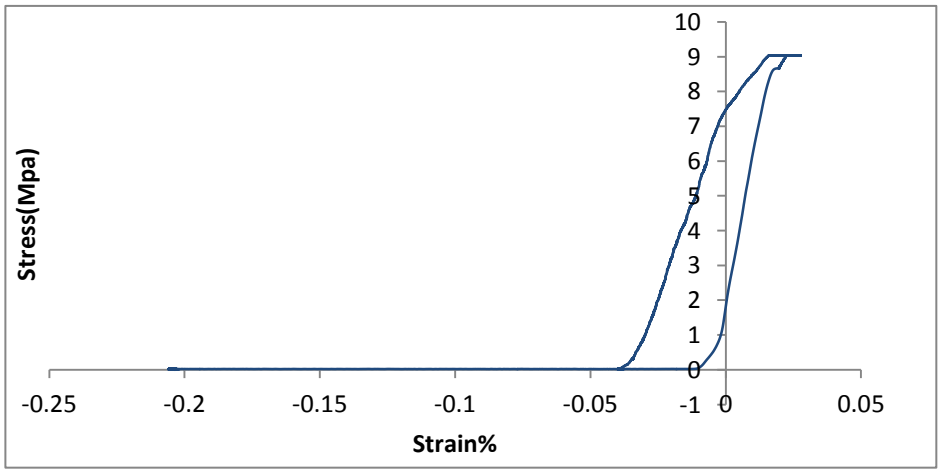

Figure 7 The stress and strain curve of homogenous scaffold

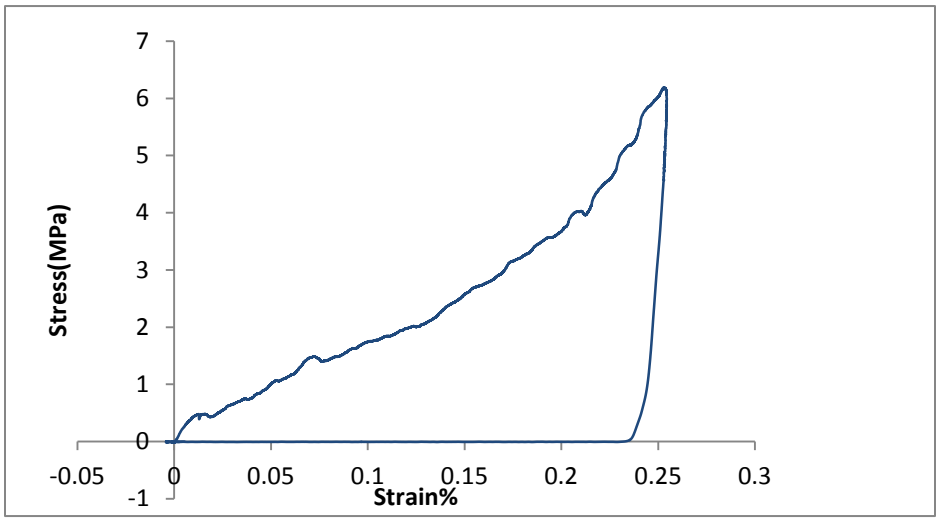

Figure 8 The stress and strain curve of gradient scaffold

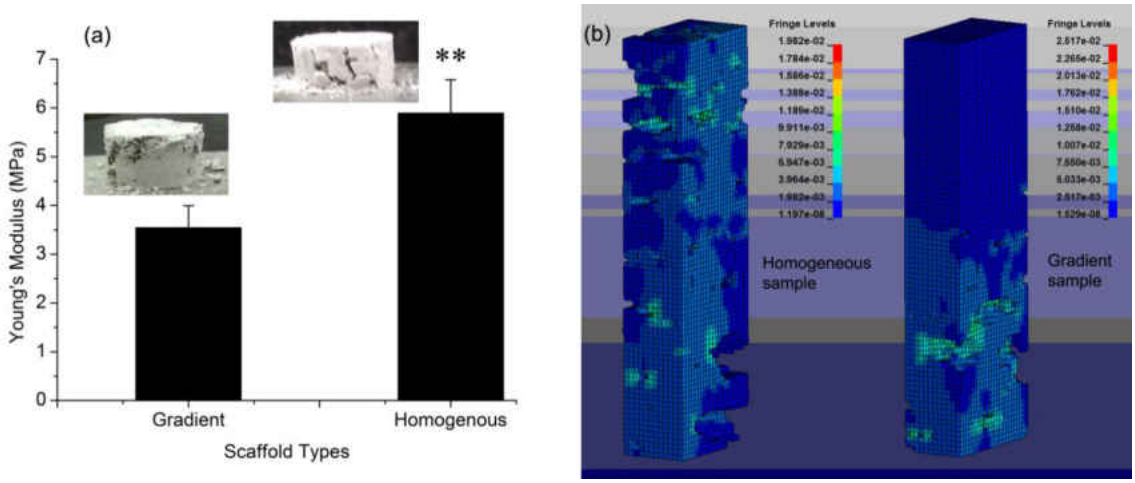

Figure 9 (a) The Young's Modulus of gradient and homogenous scaffold. (b) The distribution of stress of gradient and homogenous scaffold

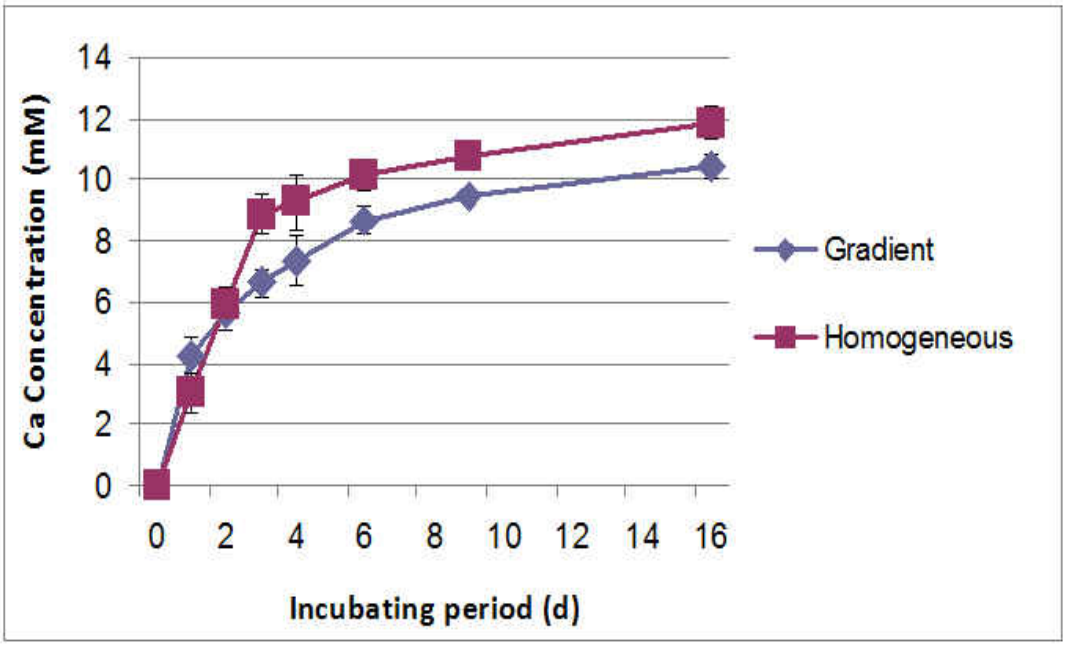

Figure 10 The degradation of gradient and homogenous

Chapter 3 Bioreactor design and condition setting

3.1 Introduction

The bioreactor is a device which use mechanism method to control and effect biological process. Compared to static cell culture, the dynamic cell culture has many advantages. Firstly, the dynamic cell culture maintains and provides ideal concentration of nutrition and oxygen through out of the scaffold [51]. It is important to the 3D scaffold because the static cell culture cannot provide enough nutrition and oxygen to the cells grown in deeper region of the 3D scaffold. Secondly, the bioreactor can enhance cellular spatial distribution [51]. Thirdly, the bioreactor provides physical stimuli. Bone cells are more sensitive to mechanical stimuli than other cells. Since muscle contraction, body movement and fluid flow can cause hydrostatic pressure, cell strain and shear stress. These mechanical stimuli stimulate cell proliferation, differentiation and increasing bone mass [52]. The bioreactor can provide shear stress through

flowed culture medium. In conclusion, the dynamic cell culture by bioreactor, better mimicked the physiological environment, is a desired approach for cell culture in tissue engineering.

The basic bioreactor should have cell culture chambers, medium reservoir, gas exchange device and power system. The cell culture condition can be controlled such as temperature, humidity, oxygen and carbon dioxide concentration and medium pH value [53]. Additionally, materials used for bioreactor should be biologically inert and noncorrosive at least. Furthermore, the physical stimuli should be controlled by flow rate or rotate rate [53]. The shear stress in bioreactor is related to flow rate, pore size, porosity and viscosity of the medium. For this reason, a desired shear stress should be calculated for different scaffold.

There are many types of bioreactor such as spinner flask bioreactor, rotating bioreactor system and perfusion bioreactor system. The main limitation of the spinner flask bioreactor and the rotating bioreactor is unevenly nutrition and shear stress distribution [54]. The perfusion bioreactor can provide more homogeneous nutrition and shear stress throughout scaffolds. Since the mechanism of the perfusion flow bioreactor is usage of a pump to force media flow through the scaffold. So it was widely used in bone tissue engineering. For example, Glowachi, *et al* seeded bone marrow stromal cells on collagen spongy scaffold and cultured by perfusion bioreactor. The results showed cells distributed on the scaffold evenly, and proliferation was better in comparison to static culture [55]. Therefore after comparison, in this study, we chose the direct perfusion flow bioreactor as the cell culture method.

3.2 Materials and Method

3.2.1 Materials

MT3T3-E1 cell line was obtained from American Type Culture Collection (ATCC) (Manassas, VA). α-Modified minimum essential medium (α-MEM) and Fetal bovine serum were purchased from Invitrogen (Carlsbad, CA). 3-(4,5-Dimethylthiazol-2-yl)-2,5-

diphenyltetrazolium bromide (MTT) assay kits was from ATCC (Manassas, VA). Pyrex round medium storage bottle, 15ml centrifuge tubes and 10ml syringe were from Sigma-Aldrich (USA). Silicon glue and epoxy purchased from Loctite (USA). Cell culture incubator was purchased from Queue Incubator (Paris, France).Silicon tubes and parts were from Nalgene and Cole-Parmer. Low oxygen gas mixture (5% oxygen, 10%carbon dioxide, balance nitrogen) was from Metro Welding (Detroit, MI). Microplate reader was obtained from BioTek (USA). Confocal Microscopy was from Leica TCS SP5 (USA).

3.2.2 Customized bioreactor preparation

3.2.2.1 Perfusion flow bioreactor design

We designed consisted of four parallel, vertically oriented cylindrical chambers, a cell culture medium reservoir, a peristaltic pump and a gas exchanger. The cell culture chamber consisted of autoclavable polypropylene plastics which were made by 15ml centrifuge tube and 10ml syringe. And a nylon cloth was placed at the middle of the chamber for supporting the scaffold. The gas exchanger was constructed by gas permeable silicone tube with five loops in the atmosphere with 5% of CO_2. After flowing out of the gas exchanger, the cell culture medium went through the chambers from top to bottom and recirculated through the chambers by peristaltic pump. The volume of culture medium used for the bioreactor system was 30ml.

3.2.2.2 Sealing method and toxicity test

Silicon glue and epoxy were chosen as glue to seal the chambers' wall and caps. Before use the cell toxicity of these materials was measured by MTT method. Briefly, there were three treatments: (1) MC3T3-E1 cells + dried silicon glue; (2) MC3T3-E1 cells + epoxy; (3) control (MC3T3-E1 cells only). Firstly, same volume of silicon glue and epoxy were coated on 24 wells plate and tried overnight. Secondly, after sterilized the plate by UV light, $2.6*10^3$ MT3T3-E1 cells were seeded in each well and cultured for 7 days. Thirdly, 20µl MTT reagent was added

into each well and incubated for 2 to 4 h until the blue crystal formazan formed. 250 µl DMSO was added as followed to dissolve the crystal formazan. Finally, the microplate reader was used to measure the color at 560nm which reflected the cell proliferation. All treatments were performed in duplicated.

3.2.2.3 Leakage test, gas exchange system test and contamination test

Assembled bioreactor was sterilized by autoclave. And the whole bioreactor filled with 30ml culture medium was stabilized by a cleaned retort stand in the cell culture incubator. Also a part of silicon tubes were connected with peristaltic pump as power to circulate the medium. The gas exchange tubes were put inside a small plastic bag (5cm x 5cm) with gas supplied. After installation, the entire bioreactor system ran for a week in order to test leakage, contamination and function of gas exchanger.

3.2.3 Perfusion condition

3.2.3.1 Gravity flow rate test

The gradient and homogenous scaffolds were installed and tightly sealed on the bottom of cut 15ml centrifuge tubes (Figure 11). In order to test the gravity flow rate of each scaffold, 10.5 ml distilled water was added into each tube. Thus the gravity flow rate (ml/min) equaled to the volume of distilled water divided by consuming time.

3.2.3.2 Theoretical calculation

The bioreactor system was used directly perfusion bioreactor. The Hagen-Poiseuille relation (τ=8 µv/ds) for laminar flow through a round conduit was applied [56]. The calculation details were list as below:

(a) τ=8 µv/ds (physiology shear stress τ: 0.8Pa-3.8Pa [57]; viscosity of cell culture medium µ: 0.77×10^{-3} Pa•s; the average diameter of pore ds: 0.21mm);

Flow rate (v): 27mm/s-129mm/s;

The average flow rate (v'): 78mm/s

(b) Area per pore: $A=\prod x\ r^2=3.46x10^{-4}\ cm^2$

(c) The volume of fluid per pore: $V=v' x\ A=2.7x10^{-3}cm^3/s$

(d) The cross section area of scaffold: $Ac=0.78cm^2$

(e) The total pore area: $At=0.78x0.32(porosity)=0.25cm^2$

(f) The number of pore: $N=At/A=726$

(g) The total volume of fluids/s: $Vt=N x V=1.96ml/s$

After cell seeding, the pore size would be narrowed. Therefore, the final flow rate should be lower than the calculated result.

The optimal amount of seeded cells is another parameter to optimize for cell culture. Generally, the total volume of seeded cell should take 20% empty space of scaffold. Based on that, the optimal amount of cells that should be seeded can be calculated. The processing was listed as followed:

(a) The total volume of the pore: gradient scaffold equaled to 0.225 cm^3; homogenous scaffold equals to 0.17472 cm^3.

(b) The average volume of pore: 0.19986 cm^3

(c) The volume of per cells: around $6.5*10^4\mu m^3$

(d) The optimal amount of seeded cell: around $5.8 *10^5$ cells

3.2.4 Cell seeding condition

3.2.4.1 Oscillating cell seeding

According to many researches, the oscillating cell seeding method results in high seeding efficiency and even cell spatial distribution [58, 59]. Therefore, we used the oscillating cell seeding method. Firstly, sterilized scaffold and bioreactor system, as well as 10ml cell suspension ($7*10^5$ cells / ml) were prepared. Secondly, in order to force the flow throughout of

the scaffold directly, the gradient and homogenous scaffolds were tightly confined in bioreactor chambers. Thirdly, culture medium was pumped (1ml/s) from top to bottom of the scaffolds for 18 seconds, and then changed the flow direction. Thus, each oscillating cycle lasted 36 seconds. The cycles were repeated 100 times and 200 times respectively. Finally, after cell seeding, the scaffolds were incubated for 2 hours. As the same, the amount of cells was tested by MTT method.

3.2.4.3 Manual cell seeding

Cell suspension with density ($2*10^6$ cells / ml) was manually pipetted to the top, bottom and side of each sterilized scaffold with 10μl droplet. Each scaffold was loaded the 300 μl cell suspension. After that, the cell seeded scaffolds were incubated for 2 hours. Also, test the cells' amount by MTT method and observe the cell's distribution by confocal microscopy.

3.2.5 Statistic Analysis

The software of SPSS will be used in the statistical analysis. The experiment results were calculated mean and standard deviation. Two tail student t test was used to analyze the results. The statistical significance (p) is 0.05.

3.3 Results

3.3.1 Customized perfusion flow bioreactor

The schematic diagram of perfusion flow bioreactor was showed in Figure 14A. And the entire bioreactor system was exhibited in Figure 14B. The four parallel chambers, medium reservoir and gas exchanger were put in the incubator. Through pressing silicon tubing by peristaltic pump, culture medium enabled to pump to the chambers from top to bottom. The chamber design was shown in Figure 12. It is composed of half 15ml centrifuge tube and half 10ml syringe. In the middle of the chamber, a nylon cloth was settled as a scaffold holder (Figure

12c). The scaffold was tightly connected with the chamber through an O-ring. The cap of chamber was drilled in the center and linked with a connecter (Figure 12b).

In the toxicity test, the cell proliferation of three treatments has no significant difference. Thus, the silicon glue and epoxy were nontoxic to cells (Figure 15). Moreover, after testing, we found only the epoxy could seal the chamber wall and cap firmly. The bioreactor system worked well. Through out of the experiment, no liquid leakage and contaminations were observed. The gas exchanger system was functional because the color of cell culture medium changed to dark orange after thirty minutes of culture.

3.3.2 Perfusion condition

In the gravity flow rate test, the gravity flow rate of homogenous scaffold was 3.425 ml/min, and the gradient scaffold was 4ml/min. Sine after cell seeding, the pore size would be narrowed. Also based on the gravity flow rate, the flow rate was set as 1ml/s. And the optimal cells' amount was $5.8*10^5$ cells.

3.3.3 Cell seeding

Compare seeding efficiency by two approaches, the amount of cells seeded on gradient scaffold by manually seeding were significantly higher than through oscillating cell seeding (100 cycles, $p=0.005$) (Figure 17). As the same, for homogenous scaffold, the efficiency of manually seeding was higher than oscillating seeding significantly (100 cycles, $p=0.013$). Increasing the cycle times did not improve the seeding efficiency, adversely, the efficiency decreased dramatically (Figure 17). While seeding method did not impact the seeding efficiency on different scaffold, for each method, the seeded cells' amount was similar on gradient and homogenous scaffold and no significant difference ($p>0.05$) (Figure 17).

Cell distribution after manually seeding was exhibited in Figure 18-19. In gradient scaffold, the cell exhibited grade distribution. Most of cells attached to the top layer, larger pore size and porosity, of the scaffold; seldom cells attached to the middle-bottom layers (Figure 18). In homogenous scaffold, cell distribution on each layer was relatively even (Figure 19).

3.4 Discussion

In order to provide similar physiological environment for cell growth, the perfusion bioreactor system was applied in this study. The perfusion bioreactor was successfully designed and able to provide dynamic culture. Its independent four chambers allowed for easy analysis each scaffold as one scaffold moved out cannot affect others. And the bioreactor system is easy to add several parallel chambers depending on experiment requirement. Besides, the assembled whole system is autoclavable together. This efficient sterilization reduces the risk of bacterial contamination. The sealing and leakage problems were crucial to this bioreactor. Silicon glue was first considered because it is non-toxic and waterproof. However, the silicon glue failed to seal the chamber's wall and cap because it is not suitable for sealing polypropylene plastics. As a result, the epoxy was chosen. Fortunately, it was non-toxic and functional. Also some parts of the bioreactor, likes tube and chamber, should be replaced after several times autoclave and cell culture, because plastic would be aging and degrade. Thus, choosing long lasting material for bioreactor is important such as glassware. Overall, the self-designed perfusion flow bioreactor system was effective, cheap and easy to fabricate.

Perfusion conditions likes flow rate and shear stress can decide cells' behavior. The flow rate is a significant parameter for cell culture, decides shear stress on cells and affects nutrition, oxygen and wastes transport. In this study, the flow rate was 1ml/s which can be accurate controlled by peristaltic pump. Also entire silicon tubes kept same inner diameter that means the

flow rate was constant through out of the bioreactor. The Hagen-Poiseuille relation for laminar flow through a round conduit was applied to calculate the flow rate. At the same time the Reynolds number ($Re=\rho vL/\mu$, ρ is the density of the fluid, v is the mean velocity of the fluid, L is travelled length of the fluid, μ is the dynamic viscosity of the fluid) was prerequisite for using Hagen-Poiseuille to identify the laminar flow. After calculation, the Re was less than 1 which meant it could be considered as laminar flow through a round conduit. Thus although the Hagen-Poiseuille relation is not accurate enough, it is suitable for this study. Besides, the shear stress formed by 1ml/s flow rate was close to 2 Pa which was in the physiology range.

Cell seeding is important for this study. The amount of seeded cells and cellular distribution were two important factors. The optimal seeded cells' volume should take 20% of the volume of total pores. Based on this principle, the total pores' volume of gradient and homogenous scaffolds were 0.225 cm^3 and 0.17472 cm^3 respectively, and there was no significant difference between two scaffolds. Therefore, the average pores' volume was used to calculate the amount of cells which is $5.8*10^5$ per scaffold. A good seeding method should keep the cell's amount and distribution evenly on each scaffold. Oscillating perfusion seeding resulted in a high seeding efficiency (70%-90%), and it distributed cells evenly throughout the scaffold [60, 61]. For this reason, static (manual) and oscillating perfusion seeding methods were tried in the study. However, the results were inversely. Not only the amount of seeded cells by oscillating seeding were significant less than the static (manual) seeding, but also the seeding efficiency of oscillating seeding (100 cycles, <10%) was much lower than the manual seeding (20%). It may because of the high flow rate for cell seeding. Since cells do not have enough time to attach to the scaffold if the flow rate is high[61], and most of the cells may finally deposit to the bottom of the bioreactor by the effect of gravity. In addition, increasing the cycle time did not

improve the seeding efficiency. Some previous research found that the high cycle number could improve cell distribution throughout of the scaffold, but also had negative effect on cell viability [62]. Besides, we designed bioreactor may not be an ideal equipment for oscillating seeding. The scaffold is better to keep inside a relative small cassette. Also cell suspension for seeding prefers to have small volume and high cell density. Since these setting can make sure that the majorities of cells pass through scaffold and reduce cells attaching the tubes of bioreactor. The other limitation of cell seeding study was that the MTT method was not the optimal method to test cells' quantity on this 3D thick, porous scaffold, because not all of formazon can be completely washed out. Therefore, the actual seeding efficiency of these methods may be higher than the results. Furthermore, for the gradient scaffold, oscillating perfusion seeding may not be suitable. Since after constant perfusion, the grade porous structure could cause most of cells deposit at the border of layer with large pore size and layer with small pore size. There are currently fewer studies being performed to investigate the effects of dynamic cell seeding onto gradient scaffolds. Therefore, in order to improve seeding efficiency, gradient scaffold cell seeding needs further study.

After manual seeding, cell distribution also observed by confocal microscopy. Each scaffold was manually divided into three layers: top (porous structure), middle, and bottom (dense structure) to observe cell distribution on each layer. On one hand, in gradient scaffold, the major cells were deposited on the top layer and the number of cells dropped from top to bottom. This proved our hypothesis that was porous layer can provided large space for cell growth. On the other hand, cells distributed evenly throughout of the homogenous scaffold. In conclusion, according to the results of MTT and confocal microscopy, we thought the manual seeding approach provided better cell growth. Besides since the seeding efficiency was low, we enhanced

the cell seeding density to $3*10^6$/ml for the next experiment. In the next part, we would compare the cell behavior on two kinds of scaffolds after dynamic cell culture.

Figure 11 The gravity flow rate test. The scaffold was tightly sealed with the tube by silicon glue.

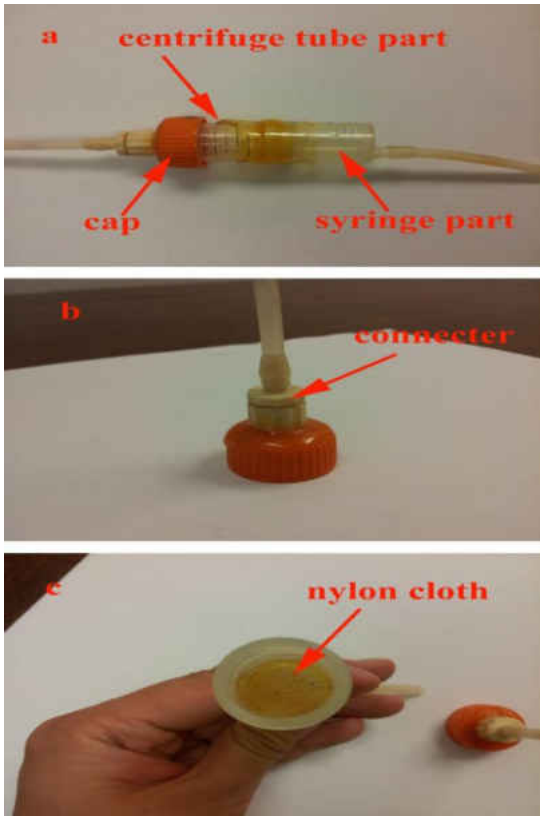

Figure 12 The chamber design. (a) The body of chamber was consisted by half centrifuge tube and half syringe. Epoxy was used to seal these two parts. (b) Gap design. (c) a nylon cloth was put in the middle of the chamber as scaffold holder.

Figure 13 Medium reservoir

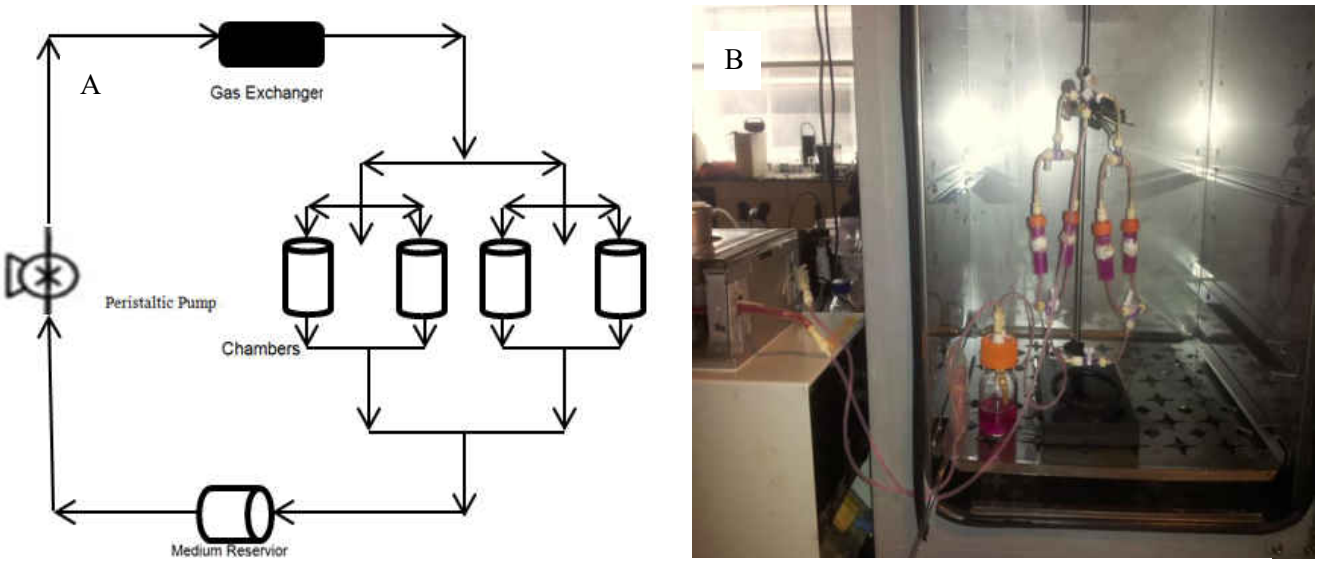

Figure 14 (A) The schematic diagram of bioreactor. (B) The perfusion flow bioreactor.

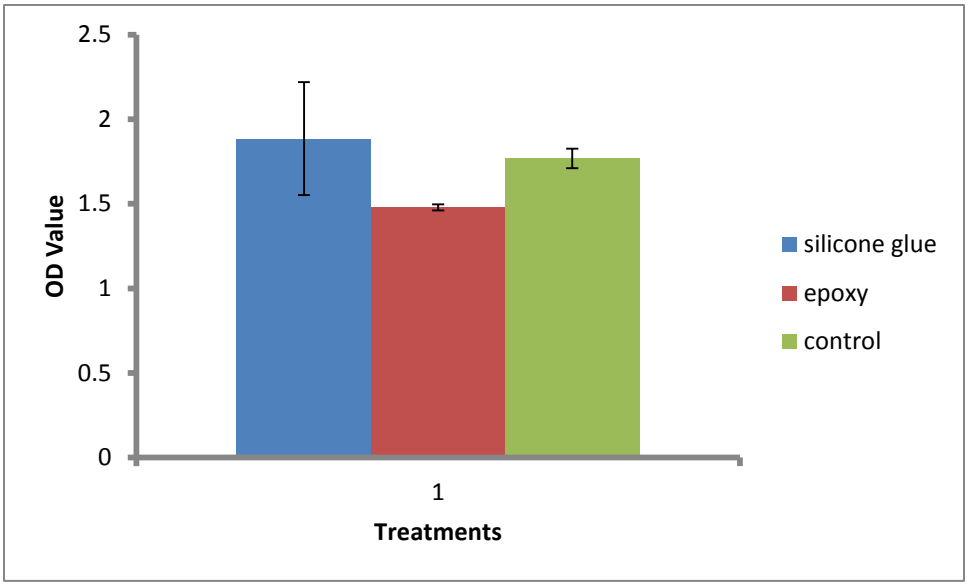

Figure 15 Toxicity test for silicone glue and epoxy

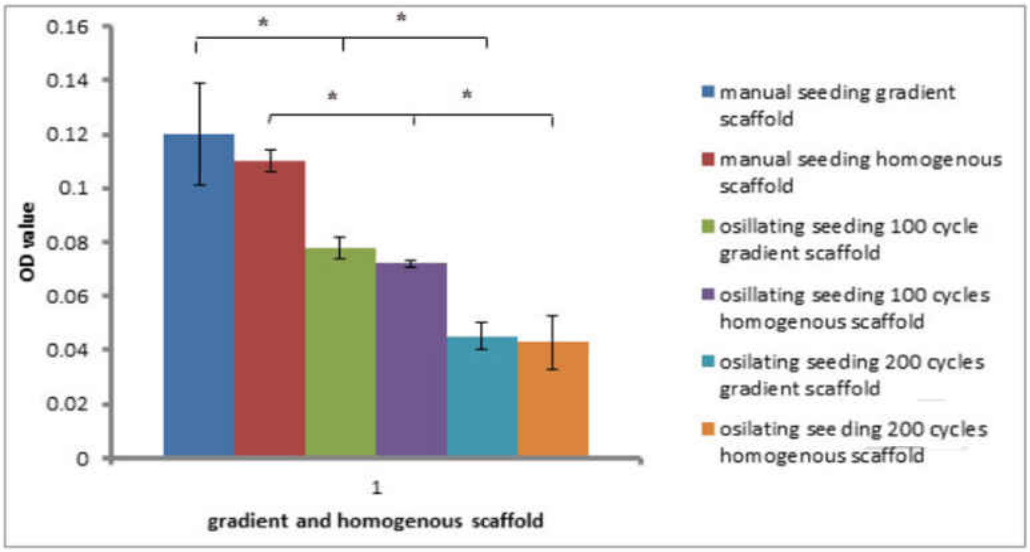

Figure 16 MTT results of cell seeding.

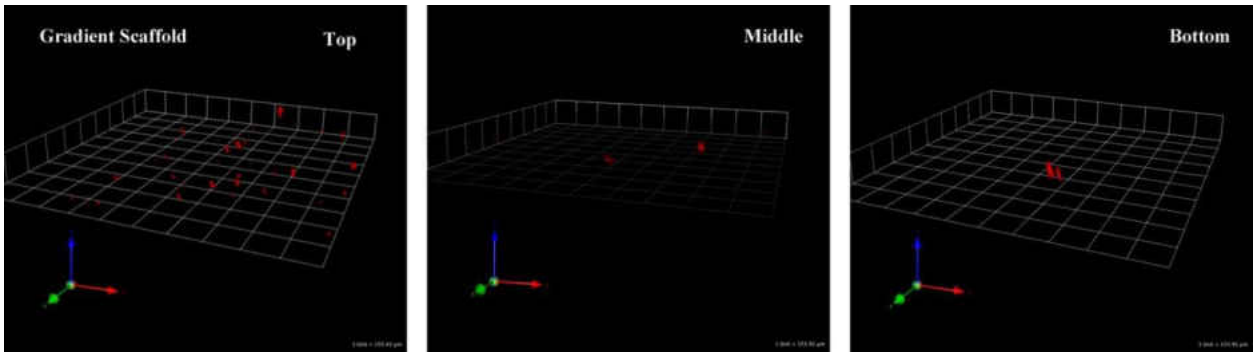

Figure 17 Cell distribution on gradient scaffold after manually seeding

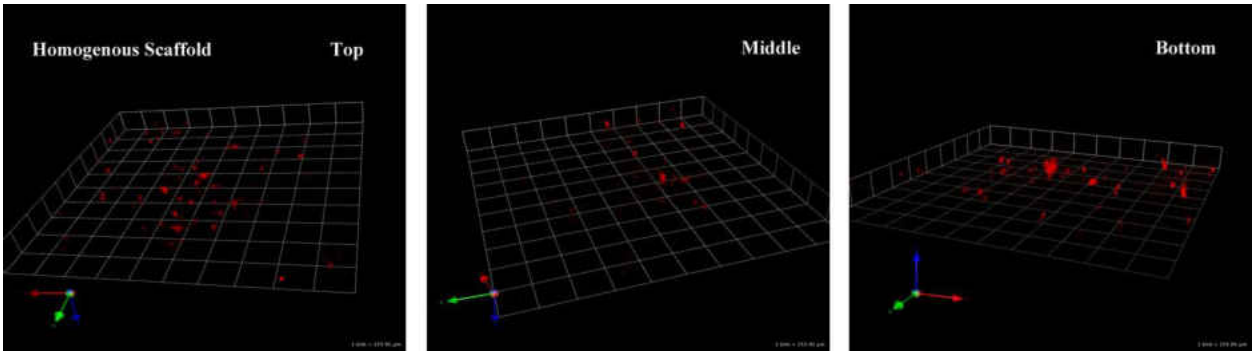

Figure 18 Cell distribution on homogenous scaffold after manually seeding

Chapter 4 In vitro comparison/evaluation of osteoblastic cell behavior between two scaffolds

4.1 Introduction

MC3T3-E1cell line, murine preosteoblasts, originates from C57BL/6 mouse calvaria and selected on the basis of high alkaline phosphatase activity. It is able to differentiate to osteoblasts and osteocytes and to form mineral deposit, hydroxyapatite. After studying the physiochemical characterization of scaffolds as well as the setting of perfusion flow cell culture, we used MC3T3-E1 cells to compare cell behavior, proliferation, distribution and differentiation, on gradient and homogenous scaffolds. We thought the gradient scaffold could improve the level of cell proliferation and differentiation, and affect the cell distribution.

4.2 Materials and Methods

MT3T3-E1 cell line was obtained from American Type Culture Collection (ATCC) (Manassas, VA). α-Modified minimum essential medium (α-MEM) and Fetal bovine serum were purchased from Invitrogen (Carlsbad, CA). 3-(4,5-Dimethylthiazol-2-yl)-2,5-diphenyltetrazolium bromide (MTT) assay kits was from ATCC (Manassas, VA). Alkaline phosphatase (AKP) assay kit was from BioVision (San Francisco, CA). Cell culture incubator was purchased from Queue Incubator (Paris, France). Microplate reader was obtained from BioTek (USA). Confocal Microscopy was from Leica TCS SP5 (USA).

4.2.1 Cell seeding and culture

MC3T3-E1 Cell (p-13) suspension with density ($3*10^6$ cells / ml) was manually pipetted to the top, bottom and side of each sterilized scaffold with 10µl droplet. Each scaffold was loaded the 300 µl cell suspension. After that, the cell seeded scaffolds were incubated overnight. The scaffolds were transformed to the perfusion bioreactor system. The cell culture condition was 37℃ with 5% of CO_2 and the culture medium was changed every two days.

4.2.2 Cell Proliferation

The cell proliferation was measured by MTT method. Briefly, after four days cell culture by the bioreactor, the cell growth scaffolds were placed in 24 well plates with 1ml culture medium. 20µl MTT reagent was added into each well and incubated for 2 to 4 h until the blue crystal formazan formed. 250 µl DMSO was added as followed to dissolve the crystal formazan. The microplate reader was used to measure the color at 560nm which reflected the cell proliferation. The MTT method was also applied after cell seeding. All measurements were performed in duplicate.

4.2.3 Cellular distribution

To observe the cell distribution on the scaffold, confocal microscopy was applied. After four days cell culture, cells grown in the scaffolds were washed by PBS for 3 times and labeled with the 250 µl Dil dye followed by incubating 15min at 37℃. After washing with PBS for 3 times, the scaffolds were measured by Leica TCS SP5 confocal microscopy to observe the cell distribution.

4.2.4 Cellular Differentiation

4.2.4.1 Pretest of cellular differentiation

In order to obtain a desire differentiation results, we designed pretest to investigate a better method to digest cells. After fourteen days static cell culture by differentiated medium, the washed samples were divided into two groups: (1) scaffolds were crushed by liquid nitrogen and then added 250µl AKP buffer to lysate cells overnight at 4℃; (2) scaffolds were added 250 µl AKP buffer directly overnight at 4℃. AKP activity in cell lysate was measured utilizing the conversion of a colorless p-nitrophenyl phosphate to a colored p-nitrophenol. The color change was measured microplate reader at 405 nm. AKP levels were converted from OD value to protein concentration based on standard curve. All measurements were performed in duplicate.

4.2.4.2 Cellular differentiation

The cell differentiation was tested by alkaline phosphatase kit (AKP). After cell seeding, the scaffolds were placed inside the bioreactor chambers. Cells were cultured by differentiated medium for fourteen days. AKP test was followed. Firstly, the scaffolds were washed by PBS for 3 times followed by centrifuge with 1000rpm for 2 min. Secondly, the scaffolds were crushed by liquid nitrogen, and then 250 µl AKP buffer was used to lysate the cells overnight at 4℃. Thirdly, AKP activity in cell lysate was measured utilizing the conversion of a colorless p-nitrophenyl phosphate to a colored p-nitrophenol. The color change was measured microplate reader at

405 nm. AKP levels were converted from OD value to protein concentration based on standard curve. All measurements were performed in duplicate.

4.2.5 Statistic Analysis

The software of SPSS was used in the statistical analysis. The experiment results were calculated mean and standard deviation. Two tail student t test was used to analyze the results. The statistical significance (p) is 0.05.

4.3 Results

4.3.1 MTT test results

After cell seeding, the amount of cells on the each scaffold was no significant difference, and the OD value was around 0.1(Figure 19). The cell proliferation shows no obviously difference no matter by static or dynamic cell culture as well (Figure 20-21). However, the cell proliferation by dynamic culture was two times higher than the cell proliferation by the static cell culture.

4.3.2 The cellular distribution images by confocal microscopy

The confocal microscopy images showed the 3D cells distribution on the scaffold. The dyed cells exhibited red dot. And the distance of unit square was around 155μm. Although the amount of grew cells were similar in the same area, the cells on the gradient scaffold (Figure 22a) grew deeper (311.8 μm) than the cell grew on the homogenous scaffold (115.9 μm) (Figure 22b).

4.3.3 The cell differentiation results by AKP test

In the pretest, although no significant difference between the two groups, the group one (crushed scaffold) had higher AKP level than the group two for both homogenous and gradient scaffolds. After dynamic culture for fourteen days, the MT3T3-E1 cells have differentiated. For the gradient scaffold, the level of cells' AKP activity (concentration) was over 1.23, which was

more than 2 times higher than the cells grown on the homogenous scaffold (Figure 24). Based on statistical analysis, the difference was significant ($P<0.01$).

4.4 Discussion

We studied cells behavior between two scaffolds after dynamic culture. Each scaffold had been seeded on same amount of cells. After cell culture for four days, the cells' proliferation has no significant difference between two kinds of scaffolds for both dynamic and static culture. According to that the graded pore structure seems do not affect the cell proliferation. The reason for that may be the total pore volume, the space for cells growth, in two kinds of the scaffolds was similar. However, when comparing the dynamic and static culture, it showed that cell proliferation by dynamic culture was two times higher than the static cell culture. It proved that the perfusion condition was suitable for MT3T3-E1 cells growth. Moreover, the bioreactor was direct medium perfusion which uses an O-ring to tightly seal the space between chamber wall and scaffold. It forces the medium flow through the scaffold and the shear stress directly transferred to the cells. Consequently, it succeeded to transport enough nutrition and oxygen through out of the scaffold and improved the efficiency of cell culture. The graded pore structure impaired the cell distribution. From the confocal microscopy image, the cells can grow deeper in the gradient scaffold as the 1^{st} and 2^{nd} layers have larger pore size and interconnectivity. This realized our design and proved our hypothesis which was the 1^{st} and 2^{nd} layers of the gradient scaffold should be responsible for cell growth.

The graded pore structure also impacted the cell differentiation. The level of AKP activity from gradient scaffold was more than two times higher than the homogenous scaffold. Thus the gradient structure did benefit to the cell differentiation. We supposed that the difference was original from the different structure of 1^{st} and 2^{nd} layers of the gradient scaffold. Since these

two layers have comparative larger pore size, higher porosity and interconnection than the homogenous one which benefit nutrition an oxygen transportation. As the results, cell can grow and develop better on 1st and 2nd layers of the gradient scaffold. Besides, the shear stress can impact cell differentiation. The shear stress on the 1st layer of gradient scaffold was 1.26 Pa which was lower than the shear stress on the homogenous one, 2.28 Pa. And both of the shear stresses were distributed in normal physiology range. However, it cannot prove our hypothesis only based on the AKP test, since it was not directly exhibited differentiated cells' location on the scaffolds. In conclusion, the gradient structure did impact the cellular distribution and enhanced the cellular differentiation level.

4.5 Limitation

Since the scaffolds we studied was a firm and thick, nontransparent structure. The traditional experimental approaches were not suitable for testing. For example, in MTT test, the formazon cannot completely washed out from the scaffolds; and in AKP test, although the scaffolds had been crushed by liquid nitrogen, it still failed to confirm that all cells was digested and cannot show the distribution of differentiated cells; also, the deepest observing distant of confocal microscopy was around 500 μm, but the scaffold had 0.8 cm in height and 1cm in width. Thus the image of confocal microscopy failed to reflex the real cell distribution. For these reasons, we applied a new labeling combined with micro-PET scanning to overcome the drawbacks.

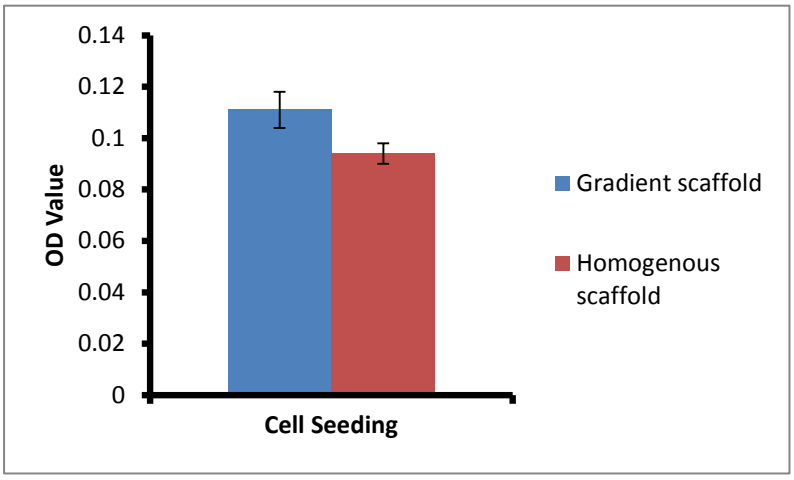

Figure 19 The amount of cells on scaffolds after cell seeding

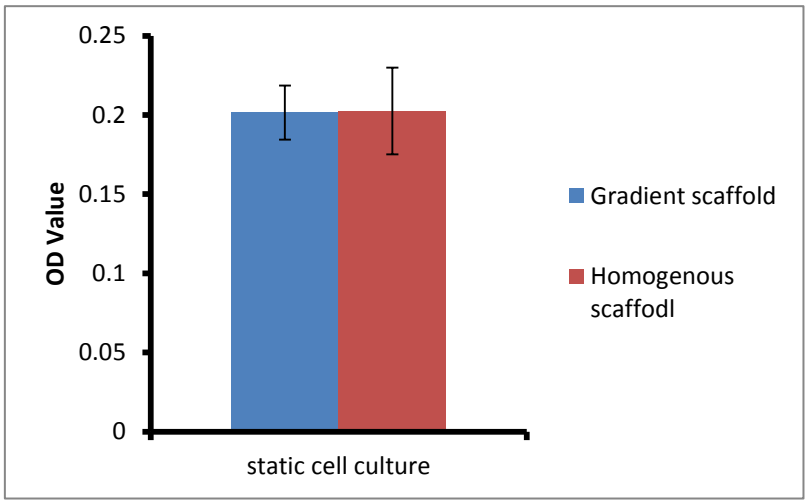

Figure 20 The cell proliferation after static cell culture

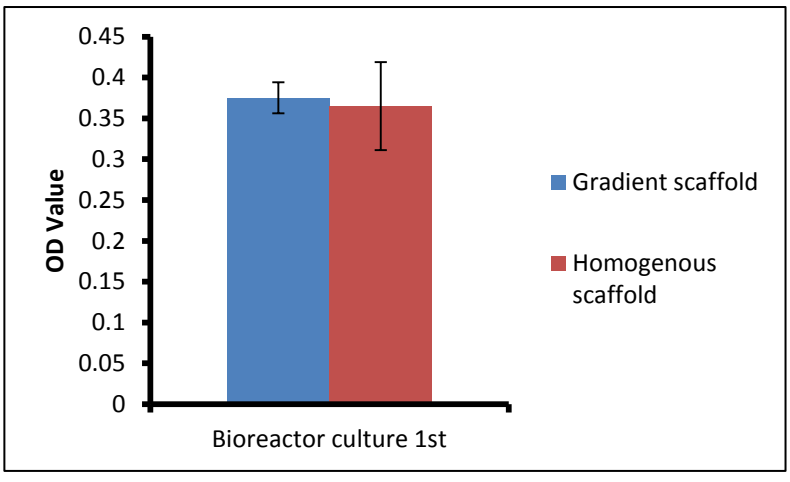

Figure 21 The cell proliferation after dynamic cell culture

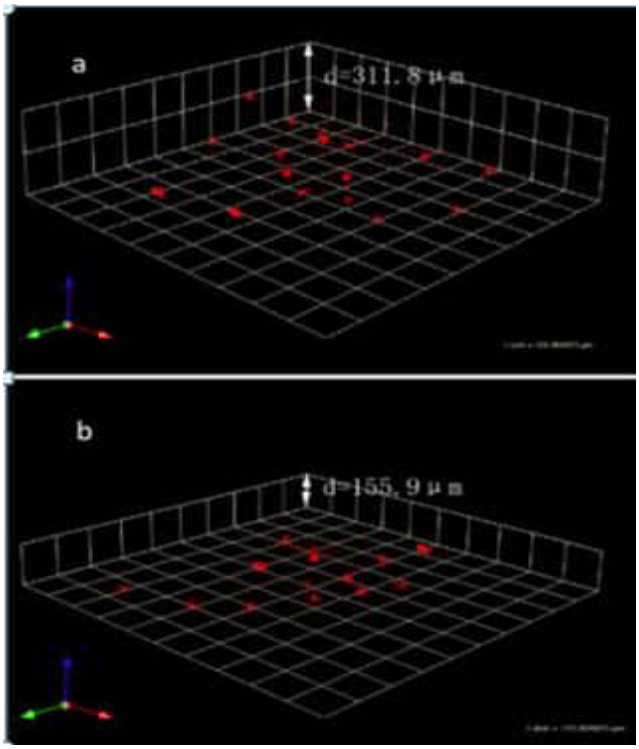

Figure 22 The cell distribution on the gradient (a) and homogenous (b) scaffold.

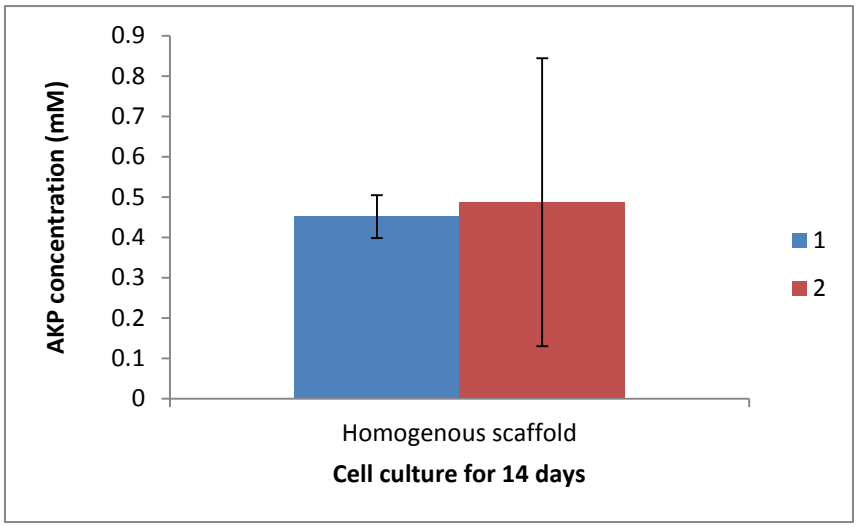

Figure 23 Pretest results of AKP. 1 was the not crushed homogenous scaffold. 2 was crushed homogenous scaffold

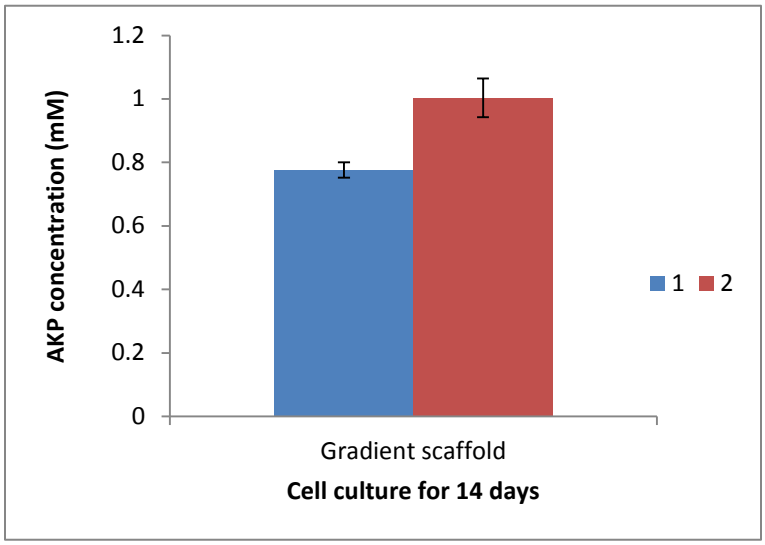

Figure 24 Pretest results of AKP. 1 was the not crushed gradient scaffold. 2 was crushed gradient scaffold

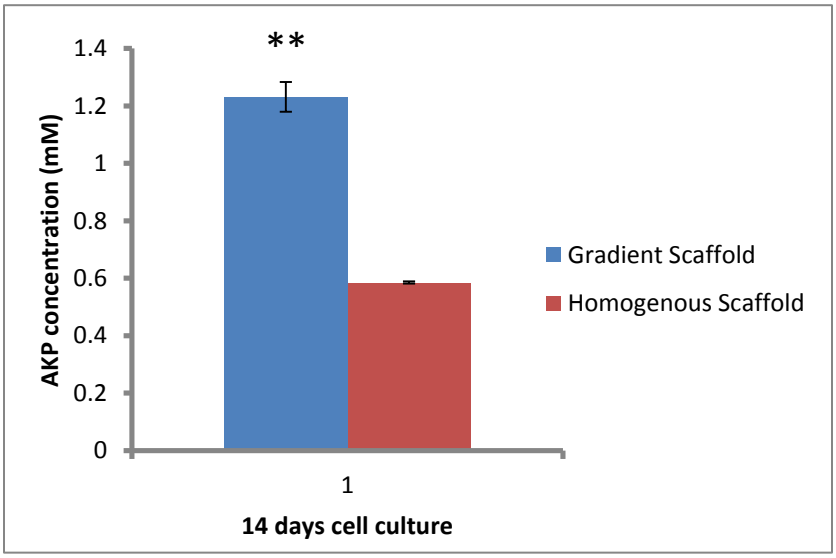

Figure 25 The results of AKP

Chapter 5 Molecular PET imaging to monitor cells growing in 3D scaffolds

5.1 Introduction

Positron emission tomography (PET) uses nuclear medical imaging technique which can detect the pairs of gamma rays emitted by a positron-emitting radionuclide, tracer, to produce a three-dimesional image or picture or functional processes in the body. PET can be used in both medical and research. In clinical, it is widely applied in oncology for diagnosis tumor. In research, PET can be used for small animal imaging which called micro-PET.

^{18}F-fluoride (^{18}F-), is a nonspecific bone tracer that has been used for skeletal imaging since the late 1960's [63]. It can diffuse through capillaries into bone extracellular fluid and exchange of fluoride ions with hydroxyapatite crystals forming fluoroapatite slowly. ^{18}F-PET is a useful tool to detect and analysis new bone forming and the healing of morselized bone allografts. Uilmark et al. used ^{18}F- PET to monitor new bone formation in periacetabular bone adjacent to the implant in 16 bilateral THA patients 1 week, 4 months and 12 months after surgery and conclude that ^{18}F- PET was an efficient tool to analysis the new bone forming [64]. In addition, ^{18}F- PET usually combines with CT to detect osteoblastic lesions.

Tetracycline (TC) has high binding affinity to hydroxyapatite (HA, $Ca_5(PO_4)_3(OH)$) through the oxygen ion on C10,C12 and C2 of TC chelate three calcium ions on HA(Figure 26) . Additionally, the calcium polyphosphate ($[Ca_2(PO_3)_4]x$ is hard to bind with TC because it has low Ca/P ratio and high steric effect based on the crystal structure (Figure 1). Therefore, TC labeling has been widely used to study bone turnover and new bone formation under normal and disease conditions[65]. When TC absorbed, it is primarily incorporate into the mineralization front of the new bone and can be detected by its fluorescence [66]. Kovar et al. recently reported near-infrared (NIR) labeled TC derivatives to be effective as markers of the bone mineralization process[67].

In this study, ^{18}F-fluoride PET technology was applied to investigate osteoblast cells' behavior and new bone forming on gradient and homogenous scaffolds. Since the ^{18}F-fluoride PET can observe and produce a 3D image based on the signal from entire scaffold. Therefore, it can overcome the limitations as mentioned above. Also fluorescent tetracycline labeling was used to detect the new forming hydroxyapatite which was able to forward reflect the differentiated level of cells and new bone forming. We hypothesized that the level of cells' differentiation and new bone forming on gradient scaffold could be higher than homogenous scaffold. Also the new formed HA may mainly deposited on the 1st and 2nd layer of gradient scaffold.

5.2 Materials and Method

5.2.1 Materials

MicroPET Rodent R4 was from Concorde Microsystems Inc.(USA), ^{18}F-fluorine solution was obtained from PET center OF Children's Hospital of Michigan, fluorescent tetracycline was from Sigma-Aldrich (USA), fluorescent microscopy (AxioCam MRc) was from Zeiss.

5.2.2 Preliminary study (wash method)

In order to find an optimal washing method, three washing conditions were designed: (1) washing scaffold three times with 150rmp (5min per time); (2) washing scaffolds five times with 150 rmp (2 min per time); (3) washing scaffolds ten times with 150 rmp (2 min per time). After soaking in FDG solution for 15min, the gradient and homogenous scaffold were washed by three different conditions, and then the scaffolds in each group were scanned by molecular PET.

5.2.3 ^{18}F-fluorine PET scanning

After culture 14 days with differentiation medium, the gradient and homogenous scaffolds were soaked in 18F-Floride medium with 150 uCi and incubated for 15 min in

incubator. After labeling, each scaffold was washed by PBS for three times. And PET scanning was used to detect the signal for 30 min.

5.2.4 Tetracycline labeling

Fluorescent labeled tetracycline is able to specific bind with the new forming hydroxyapatite (HA, $Ca_5(PO_4)_3(OH)$).The remained grounded material from AKP test was used for tetracycline labeling. All samples were stored in 1.5ml eppendorf tubes separately and avoided light for 10mins followed by washing 3times with distilled water. Finally, the material in each group was placed on glass slides and observed via fluorescence microscopy with FITH filter.

5.2.5 Statistical analysis

The software of SPSS was used in the statistical analysis. The experiment results were calculated mean and standard deviation. Two tail student t test was used to analyze the results. The statistical significance (p) is 0.05.

5.3. Results

5.3.1 Preliminary study

The three wash methods were efficient for both gradient and homogenous scaffolds. Seldom signal was detected. The first washing condition was chosen.

5.3.2 PET scanning image

The intensity of radioactivity of the scaffold was exhibited in Figure 27. The signal intensity reflected the amount of new forming HA. For the gradient scaffold (Figure 26a), the intensity of radioactivity of each layer was 3.64 $\pm$ 1.50 uCi (1st layer), 4.07 $\pm$ 0.98 uCi (2nd layer), 3.49 $\pm$ 1.31 uCi (3rd layer) and 3.12 $\pm$ 1.51 uCi (4th layer). And for the homogenous scaffold (Figure 26b), the intensity of each layer was: 3.29 $\pm$ 1.13 uCi(1st layer), 2.66 $\pm$ 1.51 uCi (2nd

layer), 2.23 ± 0.95 uCi(3rd layer), 2.23 ± 0.95 uCi (4th layer). The radioactivity of the top two layers (1st and 2nd) of the gradient scaffold was significantly intense than the radioactivity of homogenous scaffold ($P<0.05$). Also Figure 28 was a coronal image in which Figure 28a showed the radioactive intensity of gradient scaffold, and Figure 28b represented the homogenous scaffold.

5.3.3 Tetracycline labeling

Fluorescent tetracycline can only label new forming hydroxyapatite. The grounded scaffold without cells growth which was incubated in bioreactor for fourteen days as well cannot be label by fluorescent tetracycline (Figure 29a). Also for the homogenous scaffold with cell growth, the fluorescent signal was not obvious (Figure 29b). However, after fourteen days cell culture, the grounded gradient scaffold can be labeled by tetracycline (Figure 30). And clear crystal structure of hydroxyapatite was observed under the fluorescent microscopy (Figure 30b).

5.4 Discussion

In this chapter, we used ^{18}F-Fluoride PET to obtain the figure of HA distribution on the entire scaffolds. Delimiting background noise was the first step to make sure a good result of micro-PET scanning. We found that a gentle speed with rapid changing washing medium can reach an efficient washing result without affecting cells for the thick, porous structure. And finally 1st washing condition was chosen which was efficient and convenient.

The MT3T3-E1 cell line enable to differentiated into osteoblast cell and osteocytes which can form osteoid matric including hydroxyapatites (HA), calcium carbonate and calcium phosphate [2,8]. Therefore, the level of HA reflects the level of cellular differentiation. The results of micro-PET scanning showed that the HA deposition on gradient scaffold was significant higher than it on the homogenous scaffold which conformed to the AKP test. The

more important was that the image proved that HA was mainly deposited on the 1st and 2nd layer of gradient scaffold. Since the osteogenesis occurs at the area with large pore size (>350μm), high porosity and high interconnection in vivo [32]. Thus, the 1st and 2nd layers of gradient scaffold are suitable for cellular differentiation. In addition, the osteoblast and osteocytes are very sensitive to mechanical strength which induces them secreting many growth factors and promote the formation of osteoid matrix [2]. As the result, different shear stresses caused by different micro-structure of the scaffolds also impact the cellular differentiation and osteoid matrix formation. Therefore, the gradient scaffold with different functional layers was benefit to the cell differentiation and the formation of osteoid matrix. Not only did the level of differentiation on the 1st and 2nd layer on gradient scaffold was higher than its 3rd and 4th layer, but also the level of differentiation of entire gradient scaffold was higher than homogenous scaffold.

Mature osteoblast cells can secrete hydroxyapatite which is the majority inorganic component in extracellular environment of bone tissue. The fluorescent labeled tetracycline can only chelate to new forming hydroxyapatite rather than the CPP molecular because of the difference of Ca/P ratio and steric effect of these two molecular. Only in gradient scaffold, a number of new forming hydroxyapatite crystals in tetragonum had been observed. We did observed few new forming hydroxyapatites in homogenous, but they were not fully formed in tetragonum. These results directly exhibited the crystal structure of new forming HA, and proved the results of ^{18}F-Fluoride micro-PET.

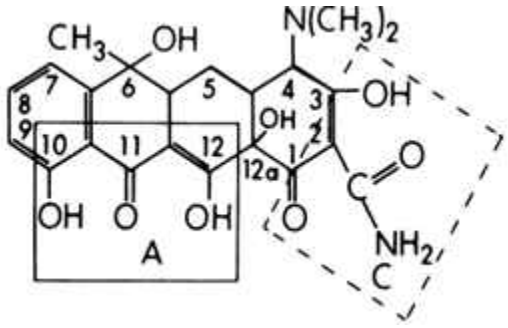

Figure 26 The chemical structure of tetracycline molecule with areas of potential calcium chelation in boxes.

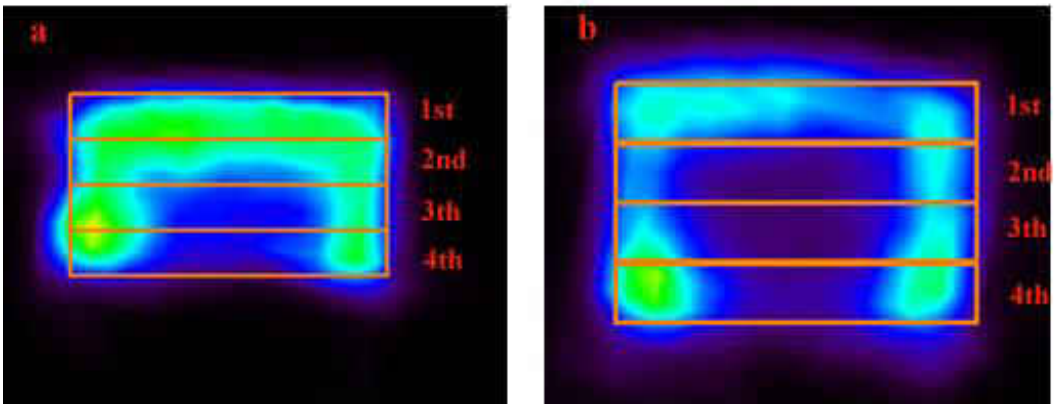

Figure 27 The intensity of radioactivity. (a) gradient scaffold (b) homogenous scaffold

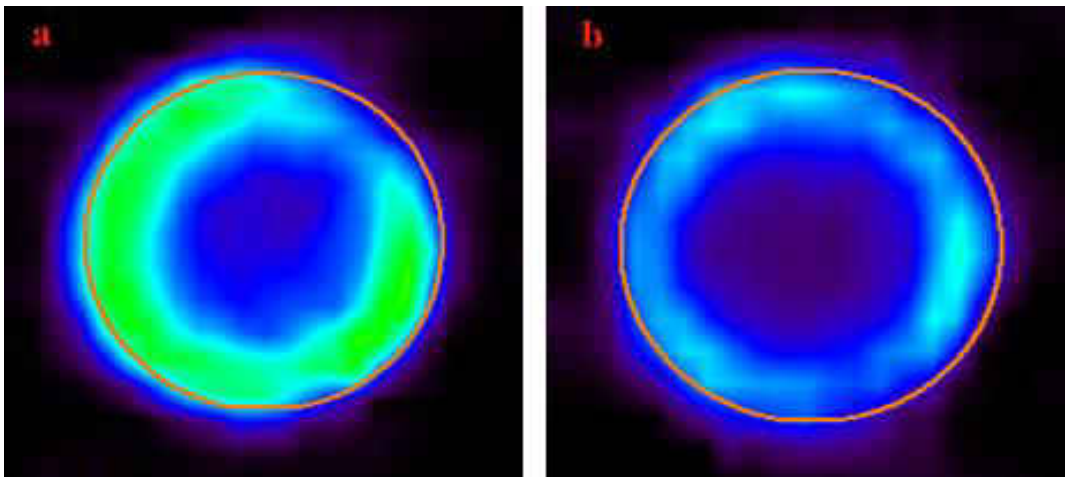

Figure 28 Coronal image of gradient (a) and homogenous (b) scaffold.

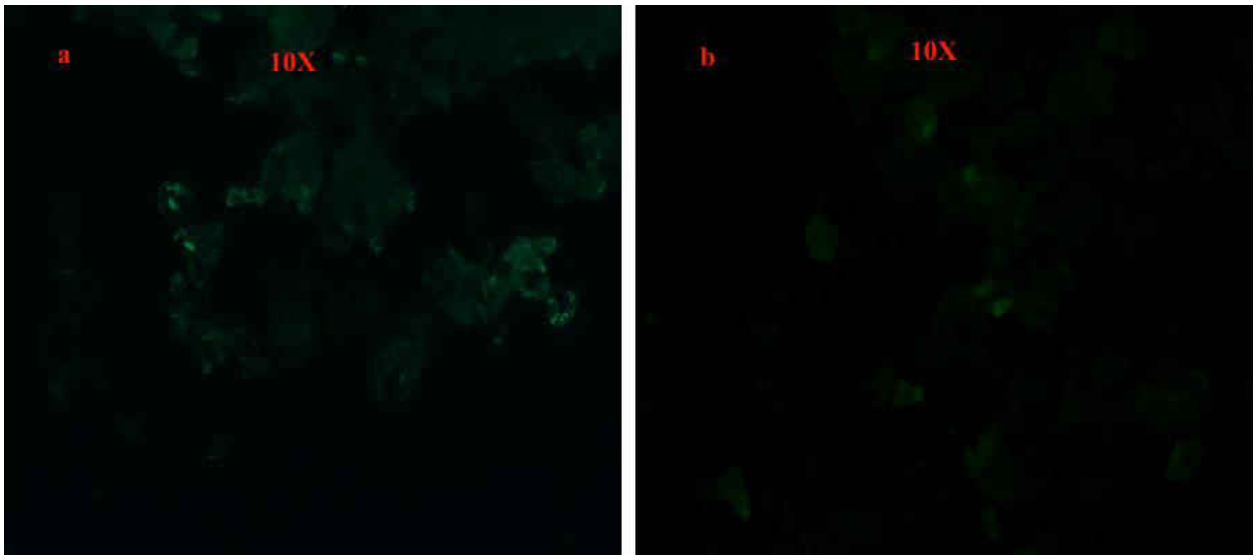

Figure 29 Fluorescent tetracycline labeling. (a) scaffold without cells (b) homogenous scaffold with cells growth

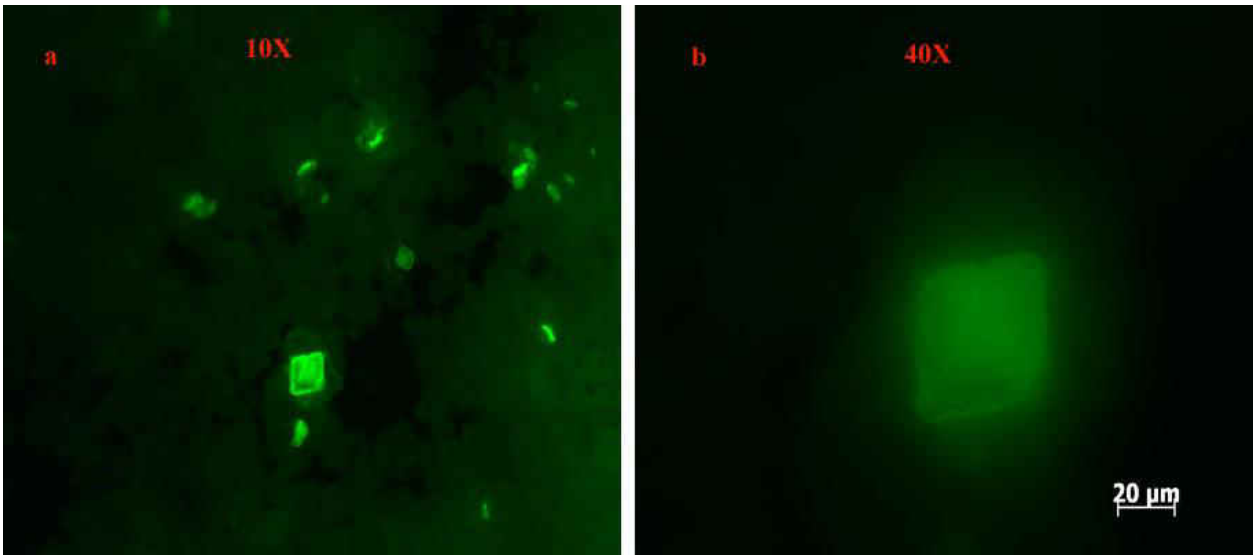

Figure 30 Fluorescent tetracycline labeling for the gradient scaffold. (a) labeled hydroxyapatite crystal on gradient scaffold (10X) (b) A single hydroxyapatite crystal (40X)

Chapter 6 Conclusions

The artificial bone grafts have been successfully applied to fix bone defects by trauma and disease. In this study, a novel calcium polyphosphate scaffold with graded pore structure was designed and developed. The gradient scaffold aimed to mimic the bone tissue morphology which has four functional layers. The porosity, degradation rate and mechanical properties had been investigated. The direct perfusion flow bioreactor was created and used in the study for cell culture. The flow rate through each scaffold was 1ml/s. It enabled to enhance cell growth and differentiation. After dynamic cell culture, in vitro cells' behavior had been compared between gradient and homogenous scaffolds through MTT method, confocal microscopy and AKP test. The gradient and homogenous scaffolds have similar empty space for cells growth. Also the results of cell proliferation showed that the amount of cells grown on each scaffold were no significant difference. However, the results appeared that the gradient structure impacted cell distribution and improved cell differentiation. Micro-PET technology was applied which can overcome the limitations of traditional method. It showed that the majority of new forming HA was deposited on the 1^{st} and 2^{nd} layer of gradient scaffold. These results proved that the different level of cell differentiation and osseous matrix forming between gradient and homogenous scaffolds did cause by the gradient structure. Therefore, the gradient scaffold has potential value of clinical application.

In future work, the mechanical strength of the gradient scaffold still needs to be improved through finer particles. For the perfusion flow bioreactor, a more durable material is necessary. Additionally, a dynamic cell seeding method for gradient scaffold is still worth to study by the bioreactor. Finally, the in vivo testing for the gradient scaffold is needed to further study the properties of the gradient scaffold.

References

1. AL., K., *Connective tissue. In:Histology and cell biology. An introduction to pathology.* St Louis: Mosby Inc, 2002: p. 118-129.
2. B, B., *From natural bone grafts to tissue engineering therapeutics: Brainstorming on pharmaceutical formulative requirements and challenges.* J Pharm Sci, 2009. **98**(4): p. 1317-75.
3. Kierszenbaum, A.L., *Histology and cell biology : an introduction to pathology*. 2002, St. Louis, Mo.: Mosby. xviii, 619 p.
4. Hall, S.J., *Basic biomechanics*. 4th ed. 2003, Boston: McGraw-Hill. xviii, 539 p.
5. Beyer Nardi, N. and L. da Silva Meirelles, *Mesenchymal stem cells: isolation, in vitro expansion and characterization.* Handb Exp Pharmacol, 2006(174): p. 249-82.
6. De Ugarte DA, M.K., Elbarbary A, Alfonso Z, Zuk PA, Zhu M, Dragoo JL, Ashjian P, Thomas B, Benhaim P, Chen I, Fraser J, Hedrick MH., *Comparison of multi-lineage cells from human adipose tissue and bone marrow.* Cell Tissues Organs, 2003. **174**(3): p. 101-9.
7. Uccelli A, F.F., Mancardi G, *Stem cells for multiple sclerosis: promises and reality.* Regen Med., 2007. **2**(1): p. 7-9.
8. Xiao Y, F.H., Prasadam I, Yang YC, Hollinger JO, *Gene expression profiling of bone marrow stromal cells from juvenile, adult, aged and osteoporotic rats: with an emphasis on osteoporosis.* Bone., 2006. **40**(3): p. 700-15.
9. Kim IS, O.F., Zabel B, Mundlos S., *Regulation of chondrocyte differentiation by Cbfa1.* Mech Dev., 1999. **80**(2): p. 159-70.
10. Ducy P, Z.R., Geoffroy V, Ridall AL, Karsenty G, *Osf2/Cbfa1: a transcriptional activator of osteoblast differentiation.* Cell, 1997. **89**(5): p. 747-54.
11. Ducy P, K.G., *Genetic control of cell differentiation in the skeleton.* Curr Opin Cell Biol, 1998. **10**(5): p. 614-9.
12. G, K., *Transcriptional regulation of osteoblast differentiation during development.* Front Biosci, 1998. **1**(3): p. 834-7.
13. Yaszemski, M.J., et al., *Evolution of bone transplantation: molecular, cellular and tissue strategies to engineer human bone.* Biomaterials, 1996. **17**(2): p. 175-85.
14. Sikavitsas, V.I., G.N. Bancroft, and A.G. Mikos, *Formation of three-dimensional cell/polymer constructs for bone tissue engineering in a spinner flask and a rotating wall vessel bioreactor.* J Biomed Mater Res, 2002. **62**(1): p. 136-48.
15. Cabraja, M. and S. Kroppenstedt, *Bone grafting and substitutes in spine surgery.* J Neurosurg Sci, 2012. **56**(2): p. 87-95.
16. Khan SN, C.F.J., Sandhu HS, Diwan AD, Girardi FP, Lane JM, *The biology of bone grafting.* J Am Acad Orthop Surg, 2005. **13**(1): p. 77-86.
17. Younger EM, C.M., *Morbidity at bone graft donor sites.* J Orthop Trauma, 1989. **3**(3): p. 192-5.
18. Gitelis, S. and P. Saiz, *What's new in orthopaedic surgery.* J Am Coll Surg, 2002. **194**(6): p. 788-91.
19. Chen, C.S., et al., *Geometric control of cell life and death.* Science, 1997. **276**(5317): p. 1425-8.
20. Flanagan, T.C., et al., *A collagen-glycosaminoglycan co-culture model for heart valve tissue engineering applications.* Biomaterials, 2006. **27**(10): p. 2233-46.
21. Hollister, S.J., *Porous scaffold design for tissue engineering.* Nat Mater, 2005. **4**(7): p. 518-24.
22. Ma, P.X. and R. Langer, *Fabrication of biodegradable polymer foams for cell transplantation and tissue engineering.* Methods Mol Med, 1999. **18**: p. 47-56.
23. Davies, J.E., *Mechanisms of endosseous integration.* Int J Prosthodont, 1998. **11**(5): p. 391-401.
24. Nojiri, C., et al., *In vivo protein adsorption on polymers: visualization of adsorbed proteins on vascular implants in dogs.* J Biomater Sci Polym Ed, 1992. **4**(2): p. 75-88.

25. Tsaryk, R., et al., *Response of human endothelial cells to oxidative stress on Ti6Al4V alloy.* Biomaterials, 2007. **28**(5): p. 806-13.
26. Valles, G., et al., *Differential inflammatory macrophage response to rutile and titanium particles.* Biomaterials, 2006. **27**(30): p. 5199-211.
27. LeGeros, R.Z., *Biodegradation and bioresorption of calcium phosphate ceramics.* Clin Mater, 1993. **14**(1): p. 65-88.
28. Sargeant, A. and T. Goswami, *Pathophysiological aspects of hip implants.* J Surg Orthop Adv, 2006. **15**(2): p. 111-2.
29. Black, J., *Systemic effects of biomaterials.* Biomaterials, 1984. **5**(1): p. 11-8.
30. D'Lima, D.D., et al., *Bone response to implant surface morphology.* J Arthroplasty, 1998. **13**(8): p. 928-34.
31. Sul, Y.T., et al., *Characteristics of the surface oxides on turned and electrochemically oxidized pure titanium implants up to dielectric breakdown: the oxide thickness, micropore configurations, surface roughness, crystal structure and chemical composition.* Biomaterials, 2002. **23**(2): p. 491-501.
32. Kuboki, Y., et al., *Geometry of artificial ECM: sizes of pores controlling phenotype expression in BMP-induced osteogenesis and chondrogenesis.* Connect Tissue Res, 2002. **43**(2-3): p. 529-34.
33. Kuboki, Y., Q. Jin, and H. Takita, *Geometry of carriers controlling phenotypic expression in BMP-induced osteogenesis and chondrogenesis.* J Bone Joint Surg Am, 2001. **83-A Suppl 1**(Pt 2): p. S105-15.
34. Thompson, I.D. and L.L. Hench, *Mechanical properties of bioactive glasses, glass-ceramics and composites.* Proc Inst Mech Eng H, 1998. **212**(2): p. 127-36.
35. Ito A, M.A., Takizawa Y, Shinkai M, Honda H, Hata K, Ueda M, Kobayashi T., *Transglutaminase-mediated gelatin matrices incorporating cell adhesion factors as a biomaterial for tissue engineering.* J Biosci Bioeng, 2003. **95**(2): p. 196-9.
36. Malafaya PB, S.G., Reis RL., *Natural-origin polymers as carriers and scaffolds for biomolecules and cell delivery in tissue engineering applications.* Adv Drug Deliv Rev., 2007. **59**(4-5): p. 207-33.
37. Rezwan, K., et al., *Biodegradable and bioactive porous polymer/inorganic composite scaffolds for bone tissue engineering.* Biomaterials, 2006. **27**(18): p. 3413-31.
38. Habraken WJ, W.J., Jansen JA., *Ceramic composites as matrices and scaffolds for drug delivery in tissue engineering.* Adv Drug Deliv Rev., 2007. **59**(4-5): p. 234-48.
39. Pilliar, R.M., et al., *Porous calcium polyphosphate scaffolds for bone substitute applications -- in vitro characterization.* Biomaterials, 2001. **22**(9): p. 963-72.
40. Thomson, R.C., et al., *Hydroxyapatite fiber reinforced poly(alpha-hydroxy ester) foams for bone regeneration.* Biomaterials, 1998. **19**(21): p. 1935-43.
41. Miao, X., et al., *Mechanical and biological properties of hydroxyapatite/tricalcium phosphate scaffolds coated with poly(lactic-co-glycolic acid).* Acta Biomater, 2008. **4**(3): p. 638-45.
42. Hench.LL., *Bioceramics.* J am Ceram Soc., 1998. **81**: p. 1705-1728.
43. Park, E.K., et al., *Cellular biocompatibility and stimulatory effects of calcium metaphosphate on osteoblastic differentiation of human bone marrow-derived stromal cells.* Biomaterials, 2004. **25**(17): p. 3403-11.
44. Fukui, H., Y. Taki, and Y. Abe, *Implantation of new calcium phosphate glass-ceramics.* J Dent Res, 1977. **56**(10): p. 1260.
45. Nelson SR, W.L., Lagow RJ, Capano PJ, Davis WL, *Evaluation of new high-performance calcium polyphosphate bioceramics as bone graft materials.* J Oral Maxillofac Surg, 1993. **51**(12): p. 1363-71.
46. Xigeng Miao, D.S., *Graded/Gradient Porous Biomaterials.* Materials, 2010. **3**: p. 26-47.

47. Oh, S.H., et al., *In vitro and in vivo characteristics of PCL scaffolds with pore size gradient fabricated by a centrifugation method.* Biomaterials, 2007. **28**(9): p. 1664-71.
48. Iwata, M.S., A.; Kishiro, K.; Kunieda, Y., *Preparation of porous hydroxyapatite materials with a continuous porosity profile by use of a filtration method.* J. Jpn. Inst. Metal, 1988. **62**: p. 1088-1094.
49. Muthutantri, A., J. Huang, and M. Edirisinghe, *Novel preparation of graded porous structures for medical engineering.* J R Soc Interface, 2008. **5**(29): p. 1459-67.
50. Rawlings, R.D., *Bioactive glasses and glass-ceramics.* Clin Mater, 1993. **14**(2): p. 155-79.
51. Bancroft, G.N., V.I. Sikavitsas, and A.G. Mikos, *Design of a flow perfusion bioreactor system for bone tissue-engineering applications.* Tissue Eng, 2003. **9**(3): p. 549-54.
52. Altman, G.H., et al., *Cell differentiation by mechanical stress.* FASEB J, 2002. **16**(2): p. 270-2.
53. Rauh, J., et al., *Bioreactor systems for bone tissue engineering.* Tissue Eng Part B Rev, 2011. **17**(4): p. 263-80.
54. Darling, E.M. and K.A. Athanasiou, *Articular cartilage bioreactors and bioprocesses.* Tissue Eng, 2003. **9**(1): p. 9-26.
55. Glowacki, J., S. Mizuno, and J.S. Greenberger, *Perfusion enhances functions of bone marrow stromal cells in three-dimensional culture.* Cell Transplant, 1998. **7**(3): p. 319-26.
56. Grayson, W.L., et al., *Effects of initial seeding density and fluid perfusion rate on formation of tissue-engineered bone.* Tissue Eng Part A, 2008. **14**(11): p. 1809-20.
57. Weinbaum, S., S.C. Cowin, and Y. Zeng, *A model for the excitation of osteocytes by mechanical loading-induced bone fluid shear stresses.* J Biomech, 1994. **27**(3): p. 339-60.
58. Weinand, C., et al., *Conditions affecting cell seeding onto three-dimensional scaffolds for cellular-based biodegradable implants.* J Biomed Mater Res B Appl Biomater, 2009. **91**(1): p. 80-7.
59. Alvarez-Barreto, J.F., et al., *Flow perfusion improves seeding of tissue engineering scaffolds with different architectures.* Ann Biomed Eng, 2007. **35**(3): p. 429-42.
60. Zhao, F. and T. Ma, *Perfusion bioreactor system for human mesenchymal stem cell tissue engineering: dynamic cell seeding and construct development.* Biotechnol Bioeng, 2005. **91**(4): p. 482-93.
61. Li, Y., et al., *Effects of filtration seeding on cell density, spatial distribution, and proliferation in nonwoven fibrous matrices.* Biotechnol Prog, 2001. **17**(5): p. 935-44.
62. Koch, M.A., et al., *Perfusion cell seeding on large porous PLA/calcium phosphate composite scaffolds in a perfusion bioreactor system under varying perfusion parameters.* J Biomed Mater Res A, 2010. **95**(4): p. 1011-8.
63. Blau, M., W. Nagler, and M.A. Bender, *Fluorine-18: a new isotope for bone scanning.* J Nucl Med, 1962. **3**: p. 332-4.
64. Ullmark, G., et al., *Bone regeneration 6 years after impaction bone grafting: a PET analysis.* Acta Orthop, 2007. **78**(2): p. 201-5.
65. Sanchez, A.R., R.S. Rogers, 3rd, and P.J. Sheridan, *Tetracycline and other tetracycline-derivative staining of the teeth and oral cavity.* Int J Dermatol, 2004. **43**(10): p. 709-15.
66. Pautke, C., et al., *Characterization of eight different tetracyclines: advances in fluorescence bone labeling.* J Anat, 2010. **217**(1): p. 76-82.
67. Kovar JL, X.X., Draney D, Cupp A, Simpson MA, Olive DM, *Near-infrared-labeled tetracycline derivative is an effective marker of bone deposition in mice.* Anal biochem., 2011. **16**(2): p. 167-73.

ABSTRACT

INVESTIGATION OF PHYSIOCHEMICAL PROPERTIES OF A NOVEL GRADIENT CALCIUM POLYPHOSPHATE BONE SCAFFOLD AND ITS INFLUENCE ON CELLULAR BEHAVIOR

By

LIANG CHEN

December 2013

Advisor: Dr. Weiping Ren

Major: Biomedical Engineering

Degree: Master of Science

A good designed bone scaffold is crucial to bone tissue engineering. We have developed and characterized a novel gradient bone scaffold by combination of Calcium Polyphosphate (CPP) with different size of porogen (stearic acids). Compared with homogenous scaffold, the gradient bone scaffold with different pore size and porosity can better mimic natural bone structure. Directly perfusion flow bioreactor was developed. This 3D dynamic cell culture was better mimic the physiological condition for cell growth. It was beneficial to nutrition and oxygen delivery throughout the whole scaffold and was able to form shear stress. We wanted to investigate the effect of the gradient structure on murine MC3T3 cells' behavior after dynamic cell culture. We hypothesize that the adhesion, proliferation and differentiation of osteogenic cells on gradient scaffolds are significantly enhanced, compared to that in homogenous scaffold.

The porosity, degradation rate and mechanical properties of gradient and homogenous scaffolds had been investigated. The total porous volume and degradation rate were similar between two scaffolds. While pore size and porosity on 1st and 2nd layer of the gradient scaffold

were higher than the homogenous scaffold, which resulted in the mechanical strength of homogenous scaffolds was higher than gradient one.

The cell proliferation (MTT method), cell distribution (confocal microscopy) and cell differentiation (Alkaline phosphatase activity) were measured. Although the level of cell proliferation on two kinds of scaffolds was similar, cell distribution and the level of cell differentiation were different between two scaffolds. On the gradient scaffold, the level of cell differentiation was two times higher than the homogenous scaffold. In order to investigate the function of each layer on the gradient scaffold, micro-PET technology was applied. The PET image showed that the majority of new forming HA was distributed on the 1^{st} and 2^{nd} layer of gradient scaffold. Also tetracycline labeling study showed the crystal structure of HA from the gradient scaffold. Therefore, the gradient scaffold with four functional layers (1^{st} and 2^{nd} for cell growth, 3^{rd} and 4^{th} for providing mechanical strength) did affect the cells' distribution and enhance the cells' differentiated which was beneficial for new bone forming.

AUTOBIOGRAPHICAL STATEMENT

EDUCATION

Graduate Education (MS)

Ph.D. of Biomedical Engineering, Wayne State University, Department of Biomedical Engineering, College of Engineering: Dr. Weiping Ren

Master of Science Biomedical Engineering, Wayne State University, Department of Biomedical Engineering. College of Engineering: Dr. Weiping Ren

Undergraduate Education (BS)

Bachelors of Science- Biotechnology, Harbin Normal University, China